

Copyright
by
Jordann Kailey Young
2015

**The Thesis Committee for Jordann Kailey Young
Certifies that this is the approved version of the following thesis:**

**Abundance, biomass and caloric content of Chukchi Sea bivalves and
influence on Pacific walrus (*Odobenus rosmarus divergens*) abundance
and distribution in the northeastern Chukchi Sea**

**APPROVED BY
SUPERVISING COMMITTEE:**

Co-Supervisor:

Kenneth H. Dunton

Co-Supervisor:

Bryan A. Black

Amber K. Hardison

**Abundance, biomass and caloric content of Chukchi Sea bivalves and
influence on Pacific walrus (*Odobenus rosmarus divergens*) abundance
and distribution in the northeastern Chukchi Sea**

by

Jordann Kailey Young, B.A.

Thesis

Presented to the Faculty of the Graduate School of

The University of Texas at Austin

in Partial Fulfillment

of the Requirements

for the Degree of

Master of Science in Marine Science

The University of Texas at Austin

May 2015

Dedication

This work is dedicated to my grandfather, Chipman Stuart, and to my brother, Kyle Thesieres, who passed on before they could see me walk the stage from the University of Texas with my Master's degree. My grandfather, who once asked a bewildered ten-year-old me which college I would be attending (then informed me that it was well past time for me to make up my mind), always encouraged me to get the best education I possibly could, to never let anyone tell me what I could and could not do, and to dedicate myself to the pursuit of knowledge. As for my brother, we lived most of our lives apart, but meeting him and learning that he shared my deep love of the ocean and all its mysteries was one of the most marvelous discoveries of my life. I'd like to think that both he and Grandpa would get a kick out of this.

Acknowledgements

First of all, I would like to thank my family: my father, who let me keep massive aquariums in his house and who supported me (emotionally *and* financially) throughout my undergraduate education and beyond; my mother, who from an early age provided me with an endless supply of marine biology books and trips to SeaWorld and Port Aransas; and my sister, my comrade-in-arms who had to listened to me ramble on about this stuff for years. I could never have achieved any of this without their love and support. I would also like to thank the captain and crew of the USCGC *Healy*, especially Gary Arndt, Kasey Dunkin and Sammy Short, for their support of all our scientific endeavors and our morale in the field. Dr. B. Konar, A. Ravelo and K. Powell of the University of Alaska Fairbanks were indispensable in their assistance in procuring bivalves from epibenthic trawls. S. Schonberg and K. Jackson provided training and support during bivalve processing, and R. Chavez and A. Fincannon of Texas Parks and Wildlife generously trained me in bomb calorimetry procedures and allowed me to use their bomb calorimeter; I certainly could not have completed this work without them. Dr. T. Connelly's statistical consultation and R-coding assistance was invaluable during the data analysis phase of this project, and Dr. E. Hersh, Dr. T. Whiteaker, and S. Jackson of the University of Texas provided critical GIS consultations when ArcGIS got rough. Walrus data were generously provided by J. Clarke of NOAA, without whom the final phase of this project could not have been completed. Finally, I would like to thank my committee

members, Ken, Bryan and Amber, for their many edits and helpful feedback, as well as my lab mates, S. Wilson, C. Bonsell, C. Harris, V. Congdon and Dr. P. Bucolo, for their help in the preparation of this thesis (and C. Bonsell in particular for being my partner-in-crime in the Arctic and beyond). This study could not have been completed without any of them.

And, because I have to, I'd like to thank my dog.

Abstract

Abundance, biomass and caloric content of Chukchi Sea bivalves and influence on Pacific walrus (*Odobenus rosmarus divergens*) abundance and distribution in the northeastern Chukchi Sea

Jordann Kailey Young, M.S. Marine Sci.

The University of Texas at Austin, 2015

Co-Supervisors: Kenneth H. Dunton, Bryan A. Black

The northeastern Chukchi Sea is a shallow subarctic shelf ecosystem that supports a significant benthic infaunal community. Bivalves are one of the dominant benthic taxa in this region, and represent a vital food resource for consumers such as Pacific walrus (*Odobenus rosmarus divergens*). The biomass, abundance and species composition of these bivalve communities not only reflect local patterns of productivity, but have the potential to affect upper trophic level consumers through bottom-up processes. Ten dominant bivalve taxa were collected over four cruises in the northeastern Chukchi Sea from 2009-2013 to establish baseline parameters in size frequency distributions, abundance, biomass and caloric content and to quantify their influence on the distribution of Pacific walrus. Pooled size-frequency distributions across all years showed strongly right-skewed distributions for most taxa, with a few showing evidence of a bimodal distribution. Calorimetric measurements revealed significant differences in caloric

density between taxa (p -value < 0.001), and whole animal wet weight was a reliable predictor of caloric content. Abundance and biomass were largely dominated by calorie-dense, deposit-feeding species, including *Macoma* spp., *Ennucula tenuis*, *Nuculana* spp. and *Yoldia* spp.. Hotspot analysis revealed areas of high abundance, biomass and calories centered on and to the southeast of Hanna Shoal. Pacific walrus abundance from June through October was generally greatest in areas of high bivalve abundance and biomass. ANOVA analysis showed significant differences in mean caloric values between areas with and without walrus present (student's t -test, p -value < 0.001), as well as between areas with low and high densities of walrus in the pooled annual dataset and in each individual month except October. The dominant bivalve taxa in this study were high-calorie deposit feeders which preferentially consume food sources that are likely to be affected by shifting sea ice dynamics, such as benthic microalgae and sea ice algae. As such, shifting sea ice dynamics have the potential to dramatically alter bivalve communities in the northeastern Chukchi Sea that may have profound implications for upper trophic levels.

Table of Contents

List of Tables	xi
List of Figures	xiv
Introduction	1
Methods.....	5
Study Area and Sampling Methods	5
Length-Weight Relationships	7
Calorimetric Analysis.....	7
Size-Frequency Distributions and Abundance, Biomass and Predicted Caloric Content of Preserved Specimens	9
Effects of Ethanol Preservation on Length-Weight Ratio.....	9
Spatial Analysis of Bivalve Abundance, Biomass and Caloric Distribution	10
Pacific Walrus Abundance and Distribution	11
Influence of Bivalve Caloric Distribution on Pacific Walrus Abundance and Distribution in Offshore Feeding Areas.....	12
Results.....	14
Length-Weight Relationships	14
Calorimetric Analysis.....	14
Size-Frequency Distributions and Abundance, Biomass and Caloric Content of Preserved Specimens.....	19
Effects of Ethanol Preservation on Length-Weight Ratio.....	19
Spatial Analysis of Bivalve Abundance, Biomass and Caloric Content	23
Pacific Walrus Abundance and Distribution	24
Influence of Bivalve Caloric Distribution on Pacific Walrus Abundance and Distribution in Offshore Feeding Areas.....	24
Discussion	34
Spatial Analysis of Bivalve Abundance, Biomass and Caloric Distribution	36

Influence of Bivalve Caloric Distribution on Pacific Walrus Abundance and Distribution in Offshore Feeding Areas.....	37
Implications of Global Change.....	39
Conclusion	44
Appendices.....	46
Appendix A	46
Appendix B	52
Appendix C	58
References.....	60
Vita	70

List of Tables

Table 1:	Mean gross heat (average international calories / gram) by taxa	16
Table 2:	Length, weight and relationship to whole animal caloric content. Based on comparison of R^2 values, weight was chosen as the parameter on which caloric predictions were based. When necessary, weight equations were fitted to the origin to avoid negative caloric predictions in small size classes; these fitted equations are noted as Adjusted Calorie Equation and Adjusted Equation R^2	17
Table 3:	Percent contribution of each taxon to abundance, biomass and caloric distribution. Taxa which were not examined in this study are denoted as “Other” and make no contribution to caloric distribution due to insufficient specimens for calorimetric analysis.....	21
Table 4:	Results of ANCOVA analysis of log-transformed length-weight ratio across all preservation years for each taxon. Significant results (p-value < 0.05) are denoted with an asterisk*.....	23
Table 5:	Pacific walrus abundance by month and results of ANOVA analysis of log-transformed mean caloric value in grid cells with different levels of walrus abundance (n = 0, 1-10, 11-100, 101-1000, and 1001+ walrus per cell). Significant results (p-value < 0.05) are denoted with an asterisk*.....	31

Table A1:	Results of multiple regressions of taxa with statistically significant differences in log-transformed length-weight ratios between years. Log-transformed length-weight ratios of each year of preservation were compared to log-transformed length-weight ratio of frozen bivalves (Year Zero) to identify significantly different years. Note that no specimens of <i>Musculus</i> spp. were collected in 2009, so no Year Five comparison was possible. Significant results (p-value < 0.05) are shown with an asterisk*.	50
Table B1:	Root mean squared errors of cross-validation comparison of interpolation techniques for abundance.	52
Table B2:	Normalized root mean squared errors of cross-validation comparison of interpolation techniques for abundance.	52
Table B3:	Root mean squared errors of cross-validation comparison of interpolation techniques for biomass.	53
Table B4:	Normalized root mean squared errors of cross-validation comparison of interpolation techniques for biomass.	53
Table B5:	Root mean squared errors of cross-validation comparison of interpolation techniques for calories.	54
Table B6:	Normalized root mean squared errors of cross-validation comparison of interpolation techniques for calories.	54
Table B7:	Root mean squared errors of cross-validation comparison of different neighborhood sizes for inverse distance weighting interpolation of abundance.	55

Table B8:	Normalized root mean squared errors of cross-validation comparison of different neighborhood sizes for inverse distance weighting interpolation of abundance.	55
Table B9:	Root mean squared errors of cross-validation comparison of different neighborhood sizes for inverse distance weighting interpolation of biomass.	56
Table B10:	Normalized root mean squared errors of cross-validation comparison of different neighborhood sizes for inverse distance weighting interpolation of biomass.	56
Table B11:	Root mean squared errors of cross-validation comparison of different neighborhood sizes for inverse distance weighting interpolation of calories.	57
Table B12:	Normalized root mean squared errors of cross-validation comparison of different neighborhood sizes for inverse distance weighting interpolation of calories.	57
Table C1:	Results of Tukey’s HSD test of gross heats across taxa (p-values). Significant results (p-value < 0.05) are denoted with an asterisk* ..	58
Table C2:	Skewness (S) and kurtosis (K) of size frequency-distributions. Taxa with insufficient sample sizes to measure skewness and kurtosis in certain years are denoted by “n/a ..	59

List of Figures

Figure 1.	A. Study area in the northeastern Chukchi Sea with Hanna Shoal outlined in black. Stations are shown in red. B. ASAMM survey transects (light blue) and grid of cells (gray) overlaid across area of ASAMM transects that intersected with the study area. Note the slightly different scales for Figures 1A and 1B.....	6
Figure 2:	Length-weight relationship of each taxon, used to extrapolate predicted weight in cases of inadequate preservation. Best-fit regression lines of length vs. weight are shown as solid lines, and R^2 values for the equations are shown on the graph. Equations of best-fit regression lines can be found in Table 2	15
Figure 3:	Gross heats of combustion (international calories per gram) by taxa with Tukey's HSD letter groupings. Note that <i>Yoldia</i> spp. has no grouping, as the mean gross heat of this taxon was significantly higher than any other taxon and consequently had no similar pairings.	16
Figure 4:	Size-frequency distributions by year for all taxa	20
Figure 5:	Weight-calorie relationships used to predict caloric content of preserved specimens. Actual measurements from bomb calorimetry specimens are shown here plotted against linear regression equations, which can be found in Table 2.	22
Figure 6:	Inverse distance weighting interpolation of abundance ($n / 0.1 \text{ m}^2$) for each individual taxon and for all taxa combined, clipped to a 60 nautical mile buffer zone surrounding the study region.	26

Figure 7:	Inverse distance weighting interpolation of biomass (g / 0.1 m ²) for each individual taxon and for all taxa combined, clipped to a 60 nautical mile buffer zone surrounding the study region.....	27
Figure 8:	Inverse distance weighting interpolation of caloric distribution (calories / 0.1 m ²) for each individual taxon and for all taxa combined, clipped to a 60 nautical mile buffer zone surrounding the study region.	28
Figure 9:	Relative contribution to total caloric content of each station by each taxon. Pie chart size is scaled to log-transformed total caloric content.	29
Figure 10:	Getis-Ord-GI* hotspot analysis of total mean abundance, biomass and calories by station. Stations with unusually high values (>2.58 standard deviations) are shown in red	30
Figure 11:	Walrus abundance and distribution in the study area in June, July, August, September, October and all months combined. Data provided by NOAA ASAMM program.	32
Figure 12:	Log-transformed mean calories per cell across various levels of walrus abundance for June, July, August, September, October and all months combined.	33
Figure A1:	Projected weights of standard lengths across all years of preservation.	51

INTRODUCTION

The Chukchi Sea, a gateway to the Arctic Ocean, supports some of the highest levels of primary production in the world (Grebmeier et al. 2006a). Primary production in the Chukchi is supported by the delivery of heat, nutrients and carbon from the Pacific Ocean by three major water masses, Anadyr Water (AW), Bering Shelf Water (BSW), and Alaskan Coastal Water (ACW, Weingartner et al. 2005, 2013). Much of this production is transferred to the benthos as a consequence of low zooplankton grazing pressure and the shallow depth of the Chukchi shelf, which limits bacterial remineralization of fixed carbon during sinking (Walsh et al. 1989, Sakshaug 2004). Thus, large amounts of organic carbon settle to the seafloor and support high levels of benthic faunal biomass, particularly in areas of the northeastern Chukchi Sea such as Hanna Shoal (Grebmeier et al. 1989, 2006a, Cooper et al. 2002, Dunton et al. 2005, Ambrose et al. 2005).

The highly productive benthic communities of Hanna Shoal are dominated by polychaetes, mollusks and crustaceans (Schonberg et al. 2014), and attract considerable numbers of benthic-feeding apex consumers to the region, including gray whales (*Eschrichtus robustus*), bearded seals (*Erignathus barbatus*), and Pacific walrus (*Odobenus rosmarus divergens*) (Feder et al. 1994, 2007, Sheffield et al. 2001, Richman and Lovvorn 2003, Lovvorn et al. 2003, Simpkins et al. 2003, Grebmeier et al. 2013). Hanna Shoal is a particularly important summer feeding ground for female and juvenile Pacific walrus, which migrate from their wintering grounds in the Bering Sea each summer to forage in the Chukchi Sea (Fay 1982, Jay et al. 2012, Schonberg et al. 2014). Though walrus feed on a wide variety of benthic organisms, analyses of stomach contents

suggest that the most frequently consumed prey items in this area are gastropods, bivalves and polychaetes (Sheffield and Grebmeier 2009).

Bivalves are one of the dominant benthic taxa in the northeastern Chukchi Sea, particularly in terms of biomass (Stoker 1978, Grebmeier et al. 1989, Feder et al. 1994, Blanchard et al. 2013, Dunton et al. 2014, Schonberg et al. 2014), and possess one of the highest caloric densities of walrus prey taxa (Wilt et al. 2013). Bivalves represent an important food resource for walrus, and walrus habitat selection in wintering grounds of the Bering Sea has been shown to be strongly influenced by the distribution of bivalve caloric biomass (Jay et al. 2014). In addition to being a direct food resource, bivalves likely support other benthic organisms that are consumed by walrus, particularly gastropods. Members of the common *Neptunea* genus are known bivalve predators (Shimek 1984), as are many congeners of Chukchi gastropods in other geographic areas (Himmelman and Hamel 1993, Scolding et al. 2007, Sato et al. 2012, Clements et al. 2013, Clements and Rawlings 2014). In addition, stable isotopes analyses and measurements of bioaccumulated mercury corroborate that Chukchi gastropods occupy a high trophic level (Fox et al. 2014, McTigue and Dunton 2014) consistent with that of a predator. As such, it is reasonable to conclude that bivalves play direct and indirect roles in walrus food webs, though these dynamics remain poorly described. In addition to their role as a food resource, bivalves play an important role in benthic communities by acting as ecosystem engineers, producing hard substrate in the form of shells that provides refuges from predation, promotes settlement of epibionts, and facilitates recruitment of their own juveniles as well as those of other species (Gutiérrez et al. 2003, Skazina et al. 2013).

Of particular concern to the Arctic Ocean and associated subarctic seas are recent warming trends and associated changes in sea ice extent and phenology of formation and

retreat, as have been documented in the northern Bering and Chukchi Seas (Meier and Stroeve 2007, Steele et al. 2008, Luchin and Panteleev 2014). These changes are projected to continue (Overland and Wang 2007, Wang and Overland 2012) and are likely to affect the magnitude, timing and location of both ice algae and phytoplankton blooms with implications for the export of energy to the benthos (Grebmeier et al. 2006b, Bluhm and Gradinger 2008) as indicated by biological responses to interannual climate variability. Overall, primary production in this region is divided between early sea-ice algae blooms and subsequent open-water pelagic productivity in the form of phytoplankton blooms (Horner and Schrader 1982, Wheeler et al. 1996, McMinn and Hegseth 2004). During cold years, a larger proportion of primary productivity occurs in the form of algae blooms along the receding sea-ice edge. During these years, low water temperatures inhibit zooplankton grazing activity (Coyle and Pinchuk 2002, Sakshaug 2004) and bacterial remineralization of primary productivity, resulting in a large portion of this fixed carbon settling to the ocean floor. During warm years, a larger proportion of primary production occurs as phytoplankton blooms in thermally stratified open waters, and the relatively warm water temperatures stimulate zooplankton grazing activity and facilitate the transfer of energy to the pelagic community at the expense of the benthic community. Studies from this region estimate that grazing can reduce exports of organic matter to the benthos by as much as 50% (Macklin et al. 2002). As such, increasing temperatures due to climate change could substantially impact benthic bivalve populations by diverting energy from benthic communities into pelagic food webs. Climate change in the Arctic is also expected to increase anthropogenic impacts from shipping, fishing and offshore oil and gas activities in the region (Huntington 2009, Harsem et al. 2011), which could increase disturbance rates for benthic communities in high-traffic shelf areas.

One of the greatest challenges facing researchers documenting the impacts of climate change on Arctic ecosystems is the lack of reliable baseline data, particularly for benthic communities (Wassmann et al. 2011). Despite the dominant role bivalves play in the benthic communities and food webs of the northeastern Chukchi Sea, these animals are poorly studied due to a lack of commercial exploitation and the logistical difficulties of conducting research in the High Arctic. To address this issue, I assessed the size frequency distribution, abundance, biomass, and caloric content of ten dominant bivalve taxa (*Astarte* spp., *Clinocardium ciliatum*, *Cyclocardia crebricostata*, *Ennucula tenuis*, *Liocyma fluctuosa*, *Macoma* spp., *Musculus* spp., *Nuculana* spp., *Serripes groenlandicus*, and *Yoldia* spp.) collected from the northeastern Chukchi Sea in 2009, 2010, 2012 and 2013. Size-frequency distributions were measured as a rough proxy of recruitment history, and size-calorie relationships were developed for each taxon and applied to produce maps of abundance, biomass, and caloric content in the Hanna Shoal region with the goal of quantifying the spatial heterogeneity of bivalve community structure. Finally, I combined maps of bivalve caloric distribution with data on the abundance and distribution of Pacific walrus in the northeastern Chukchi Sea to examine the association between walrus abundance and distribution and bivalve caloric distribution. I predicted that walrus abundance and distribution are influenced by the distribution of bivalve calories in this summer feeding area, as others have shown for Pacific walrus in Bering Sea wintering grounds (Jay et al. 2014).

METHODS

Study Area and Sampling Methods

Sampling took place in the northeastern Chukchi Sea in the area described by Chukchi Sea Oil and Gas Lease Sale 193 (Figure 1A). Quantitative samples were collected on research cruises in this region between 24 July and 12 August 2009 and 2010 aboard the research vessels *Alpha Helix* (2009) and *Moana Wave* (2010), and on Hanna Shoal between 9 August and 25 August 2012, and between 29 July and 15 August 2013 aboard the USCGC *Healy*. Stations were chosen using randomized or hexagonal tessellation techniques, and additional stations were added to fill spatial gaps, to sample areas known for historical significance or to revisit stations that had been previously sampled (see Dunton et al. 2014 for more detail). In total, bivalves were collected for abundance and biomass measurements at 90 stations across four years of sampling using a double van Veen grab (area 0.1 m²). Benthic grab samples were sieved through a 1 mm mesh screen, identified to lowest taxonomic level (genus or species) aboard ship, and preserved in 80% ethanol. In 2013, bivalves were opportunistically collected for use in bomb calorimetry from additional grabs and benthic trawls. These specimens were identified to lowest taxonomic level aboard ship and were frozen to avoid potential issues with chemical preservation altering caloric content (Benedito-Cecilio and Morimoto 2002, Hondolero et al. 2012).

Two stations were excluded from all analyses due to their remote southern location (DBO-UNT5 and Detritus), while three deep water stations from the Barrow Canyon area (BarC5, CBL16, and H111) were excluded from the abundance, biomass and caloric analyses due to their depth (>100 meters), which exceeds the generally accepted maximum foraging depth for Pacific walrus (Fay 1982, Fay and Burns 1988).

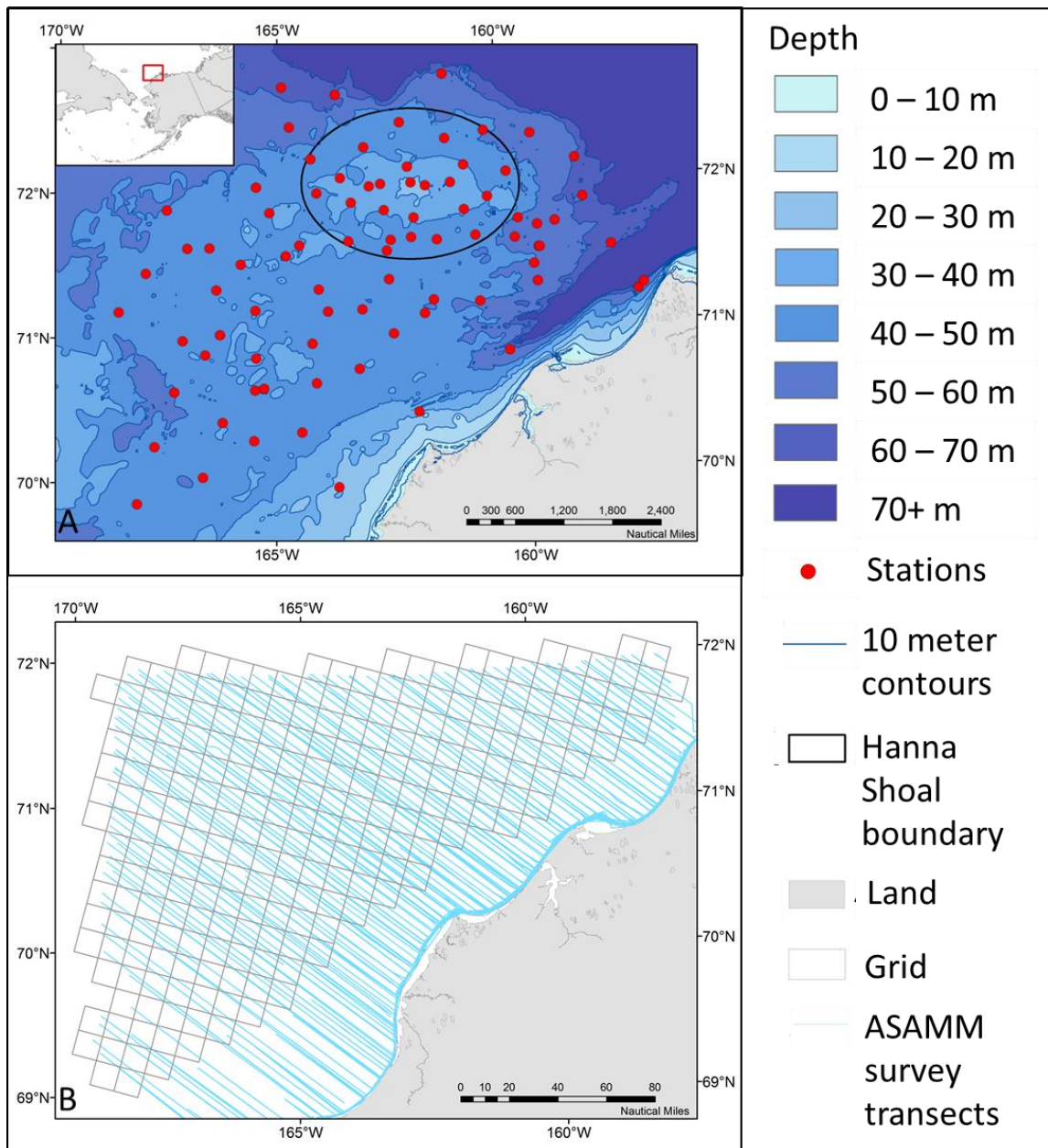


Figure 1. A. Study area in the northeastern Chukchi Sea with Hanna Shoal outlined in black. Stations are shown in red. B. ASAMM survey transects (light blue) and grid of cells (gray) overlaid across area of ASAMM transects that intersected with the study area. Note the slightly different scales for Figures 1A and 1B.

After excluding these stations, 85 stations were analyzed for abundance, biomass and caloric content, and 88 stations were analyzed for size-frequency distributions. Stations were pooled across all years to ensure adequate sample sizes for spatial analysis.

Length-Weight Relationships

Samples were transported to the University of Texas Marine Science Institute in Port Aransas, Texas, where shell lengths of frozen specimens ($n = 369$) were measured along the anterior-posterior axis to the nearest 0.1 mm, and wet weights were measured to the nearest 0.1 mg after thawing and blotting. The relationship between the length and wet weight of the frozen bivalves was determined through regression analysis. All statistics were computed using R 3.1.0 (R Core Team 2014).

Calorimetric Analysis

Frozen specimens from the 2013 Hanna Shoal cruise were analyzed for caloric content via bomb calorimetry, and length of the anterior-posterior axis and whole animal wet weight were evaluated as potential indicators of caloric content. Because feeding walrus do not consume the shells of bivalves, shells were not included in calorimetric analysis (Fay 1982). Frozen specimens were thawed and soft tissues were removed from the shells and weighed before being placed in pre-weighed tins and oven-dried at 60°C until a constant weight was achieved. After drying, the samples were re-weighed to obtain dry tissue weights for each specimen, and were homogenized and stored in a desiccator. A pellet press (Parr Instruments, Moline IL) was used to create pellets of 0.05-0.2 g, depending on the amount of homogenized tissue available from each specimen. In cases where the dry tissue weight of a specimen was of insufficient mass to be run individually, combined pellets were created by pooling similarly sized specimens that originated from the same station. In these cases, the proportional contribution of each

specimen to the combined pellet was used to determine the length and wet weight of the hypothetical combined specimen. After pooling, 308 samples were produced from the 369 specimens that were processed for bomb calorimetry. Pellet weights were recorded for each sample prior to calorimetry.

Pellets were combusted using a Model 6200 Oxygen Bomb Calorimeter (Parr Instruments, Moline IL) at the Texas Parks and Wildlife Coastal Conservation Association Marine Development Center (TPWD-CCA) in Corpus Christi, Texas. Prior to sample analysis, bombs were calibrated using a benzoic acid ($\text{C}_6\text{H}_5\text{COOH}$) pellet of approximately 0.2 grams. Caloric density was measured as gross heat of combustion, reported in international calories per gram (cal g^{-1}), and were corrected for the amount of fuse wire consumed in the combustion reaction, as well as the remaining sample weight. For some samples, a small amount of sample material remained after combustion, and the remaining sample weight was determined to be inorganic when a second round of combustion with a benzoic acid pellet failed to combust the remaining sample. The remaining sample weight was hypothesized to consist of inorganic stomach contents of bivalves (i.e. sand), as several of the bivalves in this study are classified as deposit feeders and ingest sediments during feeding (Macdonald et al. 2010).

An ANOVA was performed to test for differences in gross heat (cal g^{-1}) among taxa after log-transforming the data to meet the assumptions of homogeneity of variance (Bartlett's test $p < 0.05$). Regression analysis of wet weight and length vs. whole animal caloric content determined that weight was a better predictor of whole animal caloric content for most taxa, and thus weight was selected as the measured parameter for both size-frequency distributions and prediction of caloric content of preserved specimens.

Size-Frequency Distributions and Abundance, Biomass and Predicted Caloric Content of Preserved Specimens

Bivalves were quantitatively collected at 90 stations across all four years of sampling, and were preserved in ethanol at the time of collection. These ethanol-preserved quantitative specimens were the basis for measurements of size-frequency distributions, abundance, biomass, and caloric distribution, and specimens from all years were pooled to ensure adequate spatial coverage and sample size. Specimens were blotted and wet weight was measured to the nearest 0.1 mg for the determination of size frequency distributions, biomass and caloric content prediction. The caloric content of preserved specimens was predicted using the relationship between wet weight and whole animal caloric content obtained from bomb calorimetry for each taxon. For some preserved specimens, inadequate preservation techniques resulted in evaporation of ethanol from preservation containers, leaving the specimens desiccated. In these cases, the taxon-specific length-weight relationships developed from the frozen specimens were used to predict the wet weight of desiccated specimens, and caloric prediction was based on the predicted wet weight.

Effects of Ethanol Preservation on Length-Weight Ratio

Chemical preservation of specimens may alter specimen wet weight (Mills et al. 1982, Shields and Carlson 1996, Qureshi et al. 2008, Melo et al. 2010). Therefore, a subset of specimens from each taxon and preservation year was analyzed to determine whether preservation affected length-weight ratios. A subset of individuals that spanned the full size range for each taxon in each collection year (174-221 specimens) was analyzed for relatively abundant taxa (*E. tenuis*, *Macoma* spp., *Nuculana* spp., and *Yoldia* spp.). All available samples were analyzed for uncommon taxa (*Astarte* spp., *C. ciliatum*, *C. crebricostata*, *L. fluctuosa*, *Musculus* spp., and *S. groenlandicus*). Specimens were

measured for length along the anterior-posterior axis to the nearest 0.1 mm, and after blotting, wet weight was measured to the nearest 0.1 mg. Subsequently, a taxon-specific length-weight ratio for each preservation year was generated for comparison to the length-weight ratio generated for the frozen bivalves utilized in bomb calorimetry. The residuals did not meet the assumptions of homoscedasticity and normality, so the data were transformed using natural logarithms, which also corrected for the non-linear relationship between length and weight. After transformation, a one-way analysis of covariance (ANCOVA) was conducted with weight as the dependent variable, length as the covariate and years of preservation as the factor. Any taxon which returned at least one significantly different year was further investigated using multiple regressions to identify which year or years generated a length-weight ratio that was significantly different from the length-weight ratio of frozen specimens. In addition, for these taxa, the regressions of length vs. weight for each preserved year were used to predict the weights of standard lengths in order to determine whether the preserved specimens were predicted to be heavier or lighter at a given weight than frozen specimens (see Appendix A for additional details).

Spatial Analysis of Bivalve Abundance, Biomass and Caloric Distribution

The number of double van Veen grabs taken at each bivalve collection station was variable, so calculations of abundance, biomass and caloric values for each station were normalized to the number of grabs collected at each station. The mean abundance, biomass and caloric values of each taxon and for all taxa combined at each station were mapped using ArcGIS Version 10.1 (ESRI, Redlands, CA). Several interpolation techniques were considered for generating continuous surfaces: inverse distance weighting (IDW), completely regularized spline (CRS), spline with tension (SWT),

ordinary kriging (OK) and empirical Bayesian kriging (EBK). A cross-validation technique was used to compare the accuracy of the interpolated surface generated by each technique against the actual measured value for each station, and results were evaluated based on minimum root mean squared error (RMSE) and normalized RMSE (Tomczak 1998, Dolan et al. 2000, ESRI 2013a). In general, spline techniques outperformed the other interpolation methods in cross validation tests for the majority of taxa, but predicted negative caloric values in many areas that were considered unrealistic. Kriging techniques produced the next lowest RMSE and normalized RMSE values, but produced interpolated surfaces that typically utilized less than half of the entire range of the measured data. For these reasons, IDW was chosen as the interpolation technique for all spatial analyses. Cross-validation was also used to determine optimum neighborhood size (See Appendix B for results of cross-validation tests).

In addition to interpolation, Getis-Ord G_i^* hotspot analysis was conducted in ArcGIS for mean abundance, biomass and caloric value. Z-scores are generated for each station based on the Getis-Ord local statistic, which compares the sum of all the stations in a neighborhood to the expected neighborhood sum (ESRI 2013b, 2013c). When neighborhood sums are significantly different ($p\text{-value} < 0.1$) from the expected sum, the stations in the neighborhood are assigned statistically significant Z-scores. Significant Z-scores can be negative (indicating cold spots) or positive (indicating hotspots) (ESRI 2013b, 2013c).

Pacific Walrus Abundance and Distribution

Data on Pacific walrus distribution and abundance over the 2009-2013 study period were obtained from the annual National Oceanic and Atmospheric Administration (NOAA) Aerial Surveys of Arctic Marine Mammals (ASAMM) program. For this

program, NOAA Fisheries conducts aerial transect surveys of walrus and other marine mammals in areas of potential or current oil and natural gas development and extraction in the Chukchi and Beaufort Seas. For this study, I utilized data from survey transects in the northeastern Chukchi Sea for 2009, 2010, 2012 and 2013, and the data were pooled across years to ensure maximum spatial coverage (Figure 1B). Aerial surveys were based in Barrow and Deadhorse, AK and were conducted along offshore transects arranged perpendicular to the coast between 68°-72° N and 157°-169° W. Survey transects were offset in each year by generating a new random origin point to ensure maximum spatial coverage for multiyear datasets. Additional details on survey procedure can be found in Clarke et al. (2014), and survey data are available from the National Marine Fisheries Service National Marine Mammal Laboratory website (<http://www.afsc.noaa.gov/nmml/software/bwasp-comida.php>). Walrus data in the form of number of walrus per sighting was mapped as point data using ArcGIS (Version 10.1), and no interpolation was applied.

Influence of Bivalve Caloric Distribution on Pacific Walrus Abundance and Distribution in Offshore Feeding Areas

In order to measure the influence of bivalve caloric distribution on walrus abundance and distribution in the offshore regions of the northeastern Chukchi Sea, a grid of 238 19 km² square cells was overlaid across the region of the Lease Sale 193 area that overlapped with the ASAMM Chukchi Sea survey transects (Figure 1B). The grid was limited to offshore feeding areas and excluded coastal haulout sites that were heavily utilized by walrus in years with low sea ice (Jay et al. 2012). The size of grid cells (19 km²) was determined based on the 19 km maximum spacing between ASAMM transects. In each grid cell, the average interpolated caloric value and total walrus abundance was determined, and cells were divided into two bins based on presence or absence of walrus.

Due to the non-normal distribution of the data, the mean caloric value of cells was log-transformed prior to a pair-wise comparison of caloric values of cells in each bin using a student's t-test. Subsequently, the cells were subdivided into bins based on the total number of walrus observed in each cell (0, 1-10, 11-100, 101-1000, and 1001+ walrus per cell), and ANOVA analysis was conducted to examine the relationship between log-transformed mean bivalve calories and total walrus sightings. This analysis was conducted for the full dataset and separately for the months of June, July, August, September, and October.

RESULTS

Length-Weight Relationships

Length was an accurate predictor of weight for all taxa, returning R^2 values ranging from 0.921 (*C. crebricostata*) to 0.998 (*Yoldia* spp.), with nine out of ten taxa having R^2 values greater than 0.96 (Figure 2). The species with the weakest relationship, *C. crebricostata*, was noted to have a relatively thick periostracum with variable levels of erosion, and we hypothesized that this unaccounted-for variable might have contributed to the slightly lower R^2 value for this species.

Calorimetric Analysis

Gross heats differed significantly among taxa (ANOVA $F = 32.37$, $p\text{-value} < 0.001$), as separated by a post-hoc Tukey's Honestly Significant Difference (HSD) (Appendix, Table C1). The taxa with the highest mean gross heats were the deposit feeders *Yoldia* spp. (5661.9 ± 397.6 cal g⁻¹), *Macoma* spp. (5333.6 ± 282.9 cal g⁻¹), *Nuculana* spp. (5267.0 ± 217.7 cal g⁻¹), and *E. tenuis* (5194.1 ± 295.4 cal g⁻¹), while those with the lowest were *S. groenlandicus* and *C. crebricostata* (4715.3 ± 213.9 and 4847.8 ± 265.2 cal g⁻¹, respectively) (Table 1, Figure 3). Whole animal wet weight was found to be a robust predictor of whole animal caloric content, with R^2 values ranging from 0.76 to 0.99 (Table 2).

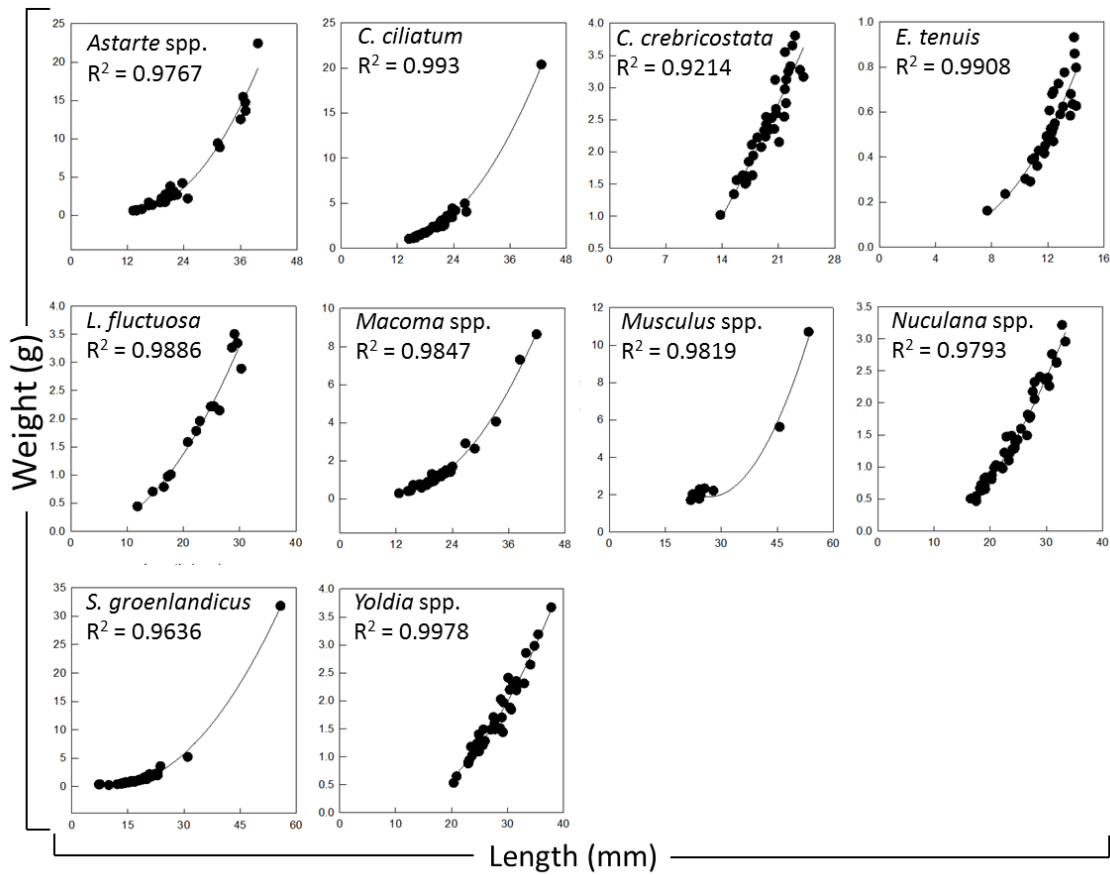


Figure 2: Length-weight relationship of each taxon, used to extrapolate predicted weight in cases of inadequate preservation. Best-fit regression lines of length vs. weight are shown as solid lines, and R^2 values for the equations are shown on the graph. Equations of best-fit regression lines can be found in Table 2

Taxon	Mean international calories / gram \pm SD
<i>Astarte</i> spp.	4929.0 \pm 264.8
<i>C. ciliatum</i>	5079.6 \pm 321.99
<i>C. crebricostata</i>	4847.8 \pm 265.2
<i>E. tenuis</i>	5194.0 \pm 295.4
<i>L. fluctuosa</i>	4971.6 \pm 229.5
<i>Macoma</i> spp.	5333.6 \pm 283.0
<i>Musculus</i> spp.	5055.5 \pm 229.6
<i>Nuculana</i> spp.	5267.1 \pm 217.7
<i>S. groenlandicus</i>	4715.3 \pm 214.0
<i>Yoldia</i> spp.	5662.0 \pm 397.6

Table 1: Mean gross heat (average international calories / gram) by taxa

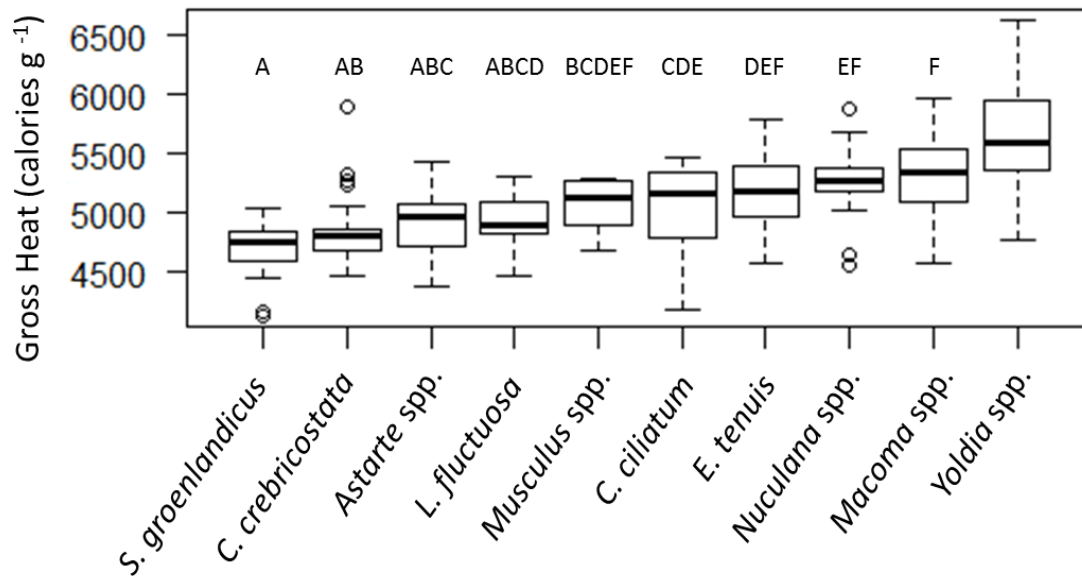


Figure 3: Gross heats of combustion (international calories per gram) by taxa with Tukey's HSD letter groupings. Note that *Yoldia* spp. has no grouping, as the mean gross heat of this taxon was significantly higher than any other taxon and consequently had no similar pairings.

Taxon	Sample Size	Length-Weight Relationship	Length v. Total Calories	R ²	Weight v. Total Calories	R ²	Adjusted Calorie Equation	R ²
<i>Astarte</i> spp.	29	W = 0.0002(L ^{3.1221})	C = 4.0918L ² - 102.68L + 949.31	0.9585	C = 161.78W + 213.04	0.9462		
<i>C. ciliatum</i>	34	W = 0.0006(L ^{2.769})	C = 15.35L ² - 438.95L + 3484.7	0.9898	C = 556.98W	0.949		
<i>C. crebricostata</i>	35	W = 0.0012(L ^{2.5366})	C = 1.4548L ^{2.0817}	0.8188	C = 277.39W + 86.118	0.8754		
<i>E. tenuis</i>	31	W = 0.0003(L ^{3.0275})	C = 0.4334L ^{2.5958}	0.6601	C = 509.36W + 24.223	0.7067		
<i>L. fluctuosa</i>	15	W = 0.001(L ^{2.3947})	C = 0.2038L ^{2.6671}	0.8765	C = 396.62W - 13.67	0.7145	C = 390.96W	0.7144
<i>Macoma</i> spp.	9	W = 0.0003(L ^{2.7313})	C = 10.51L ² - 640.35L + 10493	0.9465	C = 468.67W + 219.9	0.9469		
<i>Musculus</i> spp.	37	W = 0.0004(L ^{2.6147})	C = 2.878L ² - 22.319L + 8.0881	0.9555	C = 591.89W - 56.789	0.9625	C = 582W	0.962
<i>Nuculana</i> spp.	47	W = 0.0004(L ^{2.5441})	C = 0.1692L ^{2.5708}	0.9068	C = 389.26W + 84.289	0.9003		

Table 2: Length, weight and relationship to whole animal caloric content. Based on comparison of R² values, weight was chosen as the parameter on which caloric predictions were based. When necessary, weight equations were fitted to the origin to avoid negative caloric predictions in small size classes; these fitted equations are noted as Adjusted Calorie Equation and Adjusted Equation R².

Table 2 (continued)

<i>S. groenlandicus</i>	34	$W = 0.0007(L^{2.5864})$	$C = 5.3564L^2 - 108.86L + 716.06$	0.9966	$C = 355.36W + 99.361$	0.9928
<i>Yoldia</i> spp.	38	$W = 0.0002(L^{2.7816})$	$C = 2.1251L^2 + 17.266L - 745.93$	0.8162	$C = 836.79W$	0.866

Size-Frequency Distributions and Abundance, Biomass and Caloric Content of Preserved Specimens

Size-frequency distributions of the pooled datasets for each taxon tended to show a peaked right-skewed distribution with positive kurtosis (Figure 4; Appendix, Table B2). In addition, several taxa showed evidence of a bimodal distribution, with peaks at small and intermediate size classes. This distribution was most pronounced in *Nuculana* spp., but was also evident to a lesser degree in *Astarte* spp., *C. crebricostata*, and *Musculus* spp. (Figure 4).

The most numerically dominant taxa in the study area were *E. tenuis* (37.9%) and *Macoma* spp. (25.5%), followed by *Nuculana* spp. (13.7%) and *Yoldia* spp. (10.6%, Table 3). In terms of biomass, *Macoma* spp. (36.9%) was the dominant taxon, followed by *Nuculana* spp. (16.8%), *E. tenuis* (14.4%), and *Astarte* spp. (9.1%, Table 3). Caloric content was calculated using taxon-specific weight-calorie relationships (Figure 5), and *Macoma* spp. (45.8%), *E. tenuis* (14.8%), *Nuculana* spp. (13.9%), and *Yoldia* spp. (9.8%) dominated the caloric distribution (Table 3).

Effects of Ethanol Preservation on Length-Weight Ratio

ANCOVA analysis resulted in four taxa (*C. ciliatum*, *Macoma* spp., *S. groenlandicus* and *Yoldia* spp.) showing no significant differences in length-weight ratios between preserved specimens and frozen specimens, while the remaining six (*Astarte* spp., *C. crebricostata*, *E. tenuis*, *L. fluctuosa*, *Musculus* spp. and *Nuculana* spp.) returned at least one preserved year with a significantly different length-weight ratio from that of frozen specimens (Table 4). Due to a lack of clear patterns of weight gain or loss in these taxa, the application of a correction factor was not considered justified (see Appendix A for more details).

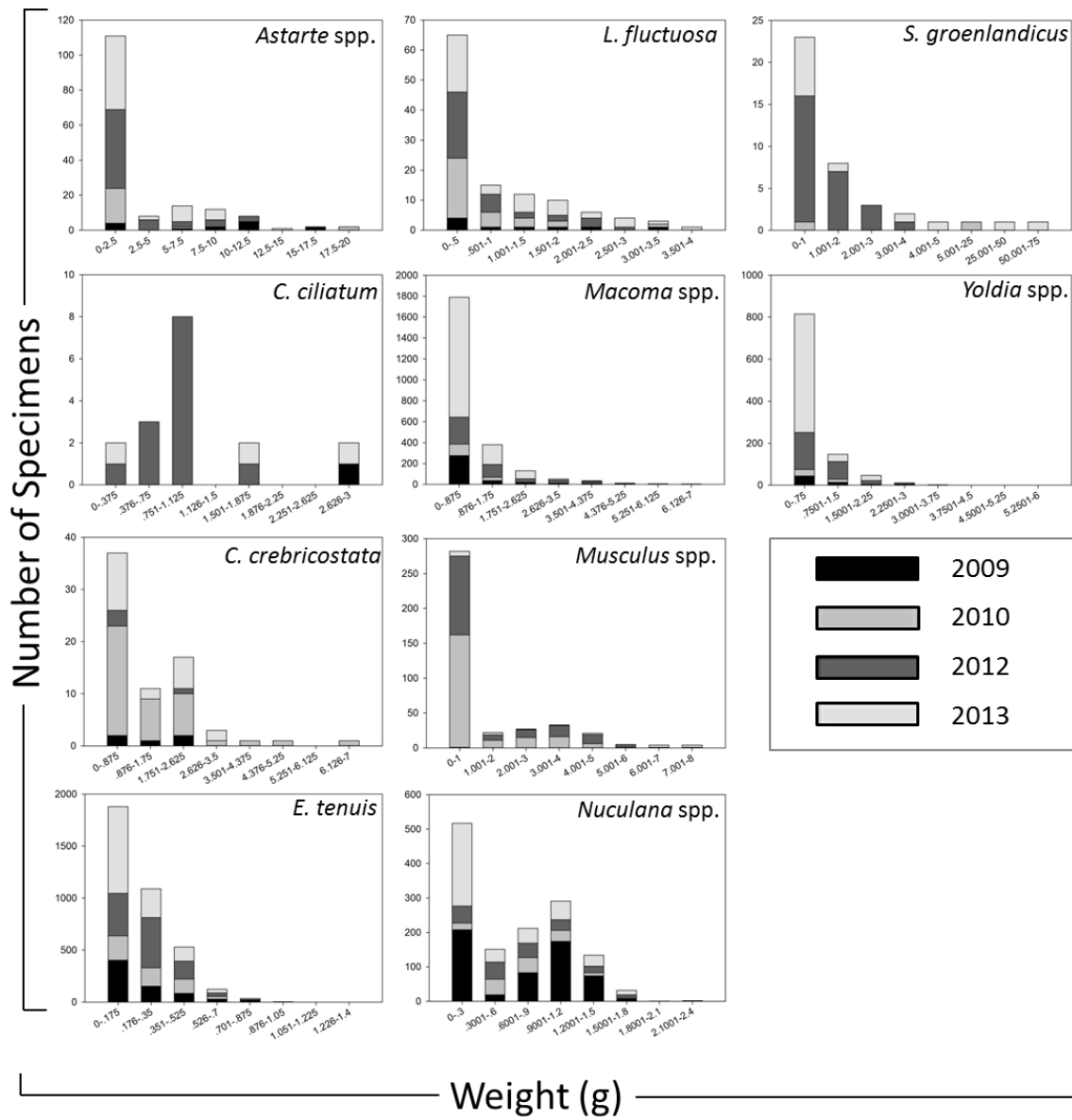


Figure 4: Size-frequency distributions by year for all taxa

Taxa	% Total Mean Abundance	% Total Mean Biomass	% Total Mean Calories
<i>Astarte</i> spp.	1.6	9.1	3.5
<i>C. ciliatum</i>	0.1	0.3	0.3
<i>C. crebricostata</i>	0.8	1.7	1.0
<i>E. tenuis</i>	37.9	14.4	14.8
<i>L. fluctuosa</i>	1.2	1.8	1.1
<i>Macoma</i> spp.	25.5	36.9	45.8
<i>Musculus</i> spp.	4.1	8.4	7.9
<i>Nuculana</i> spp.	13.7	16.3	13.9
<i>S. groenlandicus</i>	0.5	3.3	2.1
<i>Yoldia</i> spp.	10.6	7.3	9.8
Other	4.1	0.5	0

Table 3: Percent contribution of each taxon to abundance, biomass and caloric distribution. Taxa which were not examined in this study are denoted as “Other” and make no contribution to caloric distribution due to insufficient specimens for calorimetric analysis.

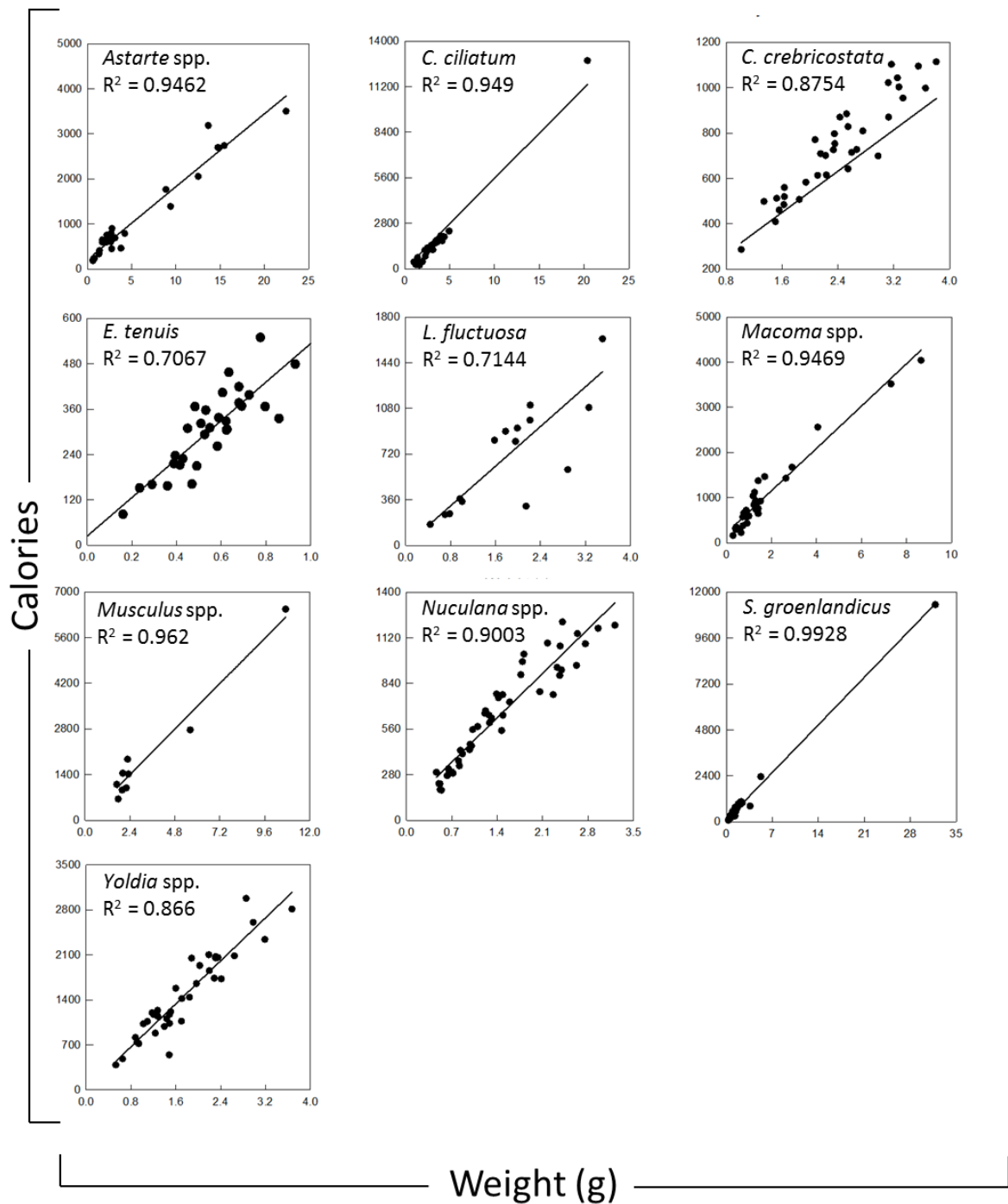


Figure 5: Weight-calorie relationships used to predict caloric content of preserved specimens. Actual measurements from bomb calorimetry specimens are shown here plotted against linear regression equations, which can be found in Table 2.

Taxon	F	p-value
<i>Astarte</i> spp.	4.5153	0.001734*
<i>Clinocardium ciliatum</i>	2.8361	0.068516
<i>Cyclocardia crebricostata</i>	8.8359	3.986e-06*
<i>Ennucula tenuis</i>	3.3144	0.01123*
<i>Liocyma fluctuosa</i>	9.5349	1.027e-06*
<i>Macoma</i> spp.	0.9611	0.43
<i>Musculus</i> spp.	10.711	1.688e-06*
<i>Nuculana</i> spp.	6.340	6.854e-05*

Table 4: Results of ANCOVA analysis of log-transformed length-weight ratio across all preservation years for each taxon. Significant results (p-value < 0.05) are denoted with an asterisk*

Spatial Analysis of Bivalve Abundance, Biomass and Caloric Content

Bivalves were present throughout the study area and were found at 76 of the 90 stations sampled, but individual taxon distributions were spatially heterogeneous (Figure 6-9). Four taxa (*C. ciliatum*, *C. crebricostata*, *Musculus* spp. and *S. groenlandicus*) were relatively rare throughout the study area, and were found at less than a quarter of all stations (7, 17, 13 and 16 stations), while *Astarte* spp. and *L. fluctuosa* were moderately common, occurring at 35 and 40 stations respectively. The remaining taxa (*E. tenuis*, *Macoma* spp., *Nuculana* spp. and *Yoldia* spp.) were extremely common and were found at over half of all stations (71, 66, 54 and 52). As a result, clusters of stations with caloric compositions that were dominated by a single taxon were common (Figure 9). Stations that were calorically dominated by *Nuculana* spp. were found predominantly in the western portion of the study region, while *Macoma* spp. dominated stations surrounding Hanna Shoal, and a few stations with high biomass of *Musculus* spp. were found in the region to the east of the shoal near Barrow Canyon.

In general, the interpolated maps showed that areas of highest abundance, biomass and caloric content occurred on Hanna Shoal and in regions to the south and east of the shoal (Figures 6-8), which was confirmed by hotspot analysis (Figure 10). Maps of

biomass and caloric distribution also showed an area of high biomass and caloric density in the western portion of the study area (Figures 7, 8), which was due to an unusually high biomass of *Nuculana* spp. collected at one station in one year. However, because this high biomass and caloric content was only measured at one station, it was not classified as a hotspot and was not reflected in the hotspot analysis maps (Figure 10).

Pacific Walrus Abundance and Distribution

Pacific walrus abundance in the study area was highest during July and August, with intermediate abundances in June and September, and the lowest abundances in October (Table 5, Figure 11). When the annual dataset was examined visually, the largest aggregations of walrus in offshore areas were concentrated on Hanna Shoal (Figure 11). Large numbers of walrus were also observed along the Alaskan coastline in September (Figure 11), which was due to heavy utilization of coastal haulout sites during times of low sea ice availability (Jay et al. 2012). However, these coastal haulout areas were excluded from the present study, which focuses on walrus distribution in offshore feeding areas.

Influence of Bivalve Caloric Distribution on Pacific Walrus Abundance and Distribution in Offshore Feeding Areas

Significant differences were found in the mean caloric value of cells where walrus were present vs. cells where they were absent (student's t-test, $t = -5.7437$, $df = 235.78$, $p\text{-value} < 0.001$). ANOVA analysis of total walrus abundance and log-transformed mean caloric value per cell returned significant results for the annual dataset as well as all individual months except October (Table 5). The strongest correlations between log-transformed mean caloric values and walrus abundance were observed in July ($F = 20.85$, $p\text{-value} = 1.03e-14$), August ($F = 32.85$, $p\text{-value} < 2e-16$), and in the annual dataset ($F =$

28.48, $p\text{-value} < 2e-16$). In general, high mean caloric values were correlated with high densities of Pacific walrus (Figure 12).

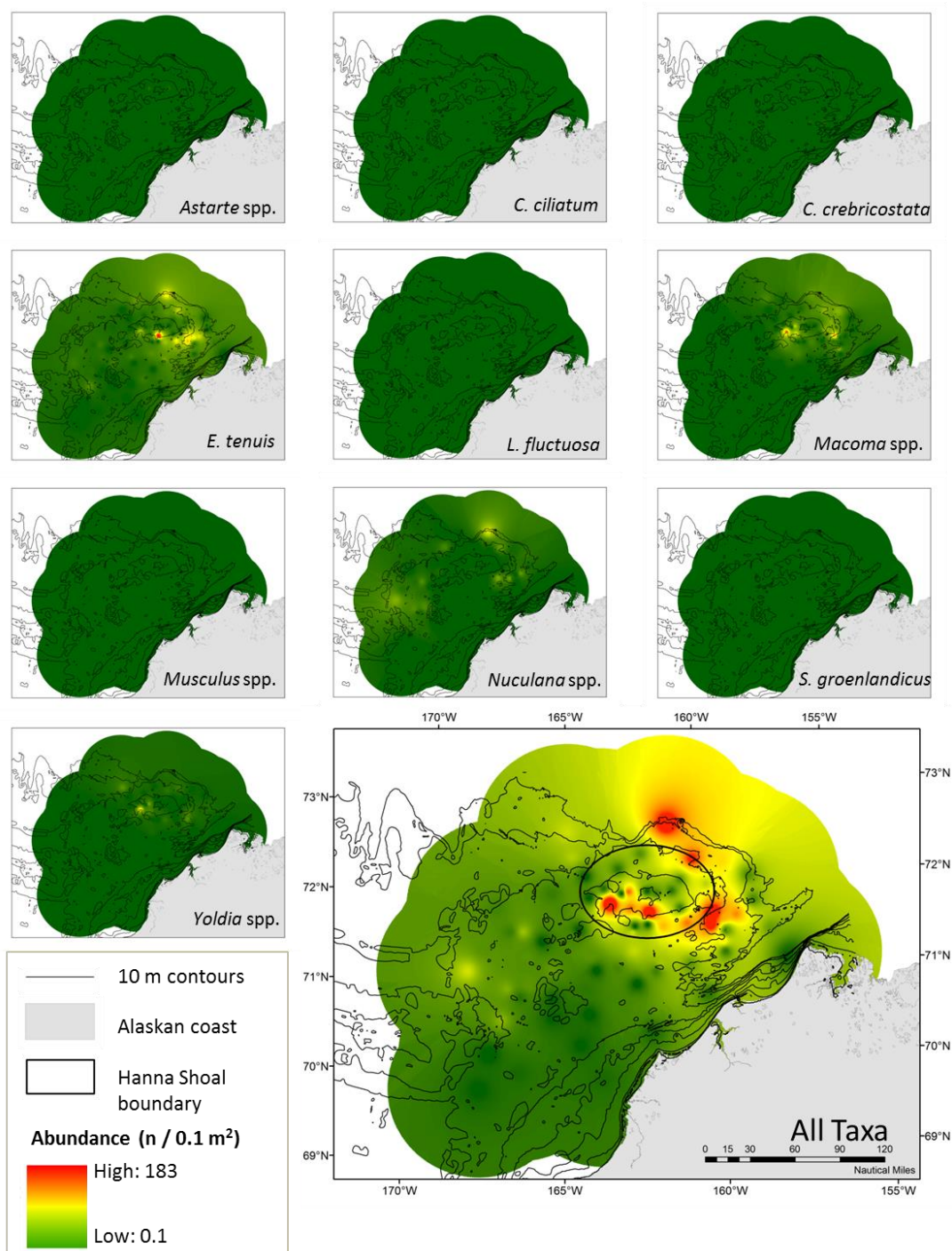


Figure 6: Inverse distance weighting interpolation of abundance (n / 0.1 m²) for each individual taxon and for all taxa combined, clipped to a 60 nautical mile buffer zone surrounding the study region.

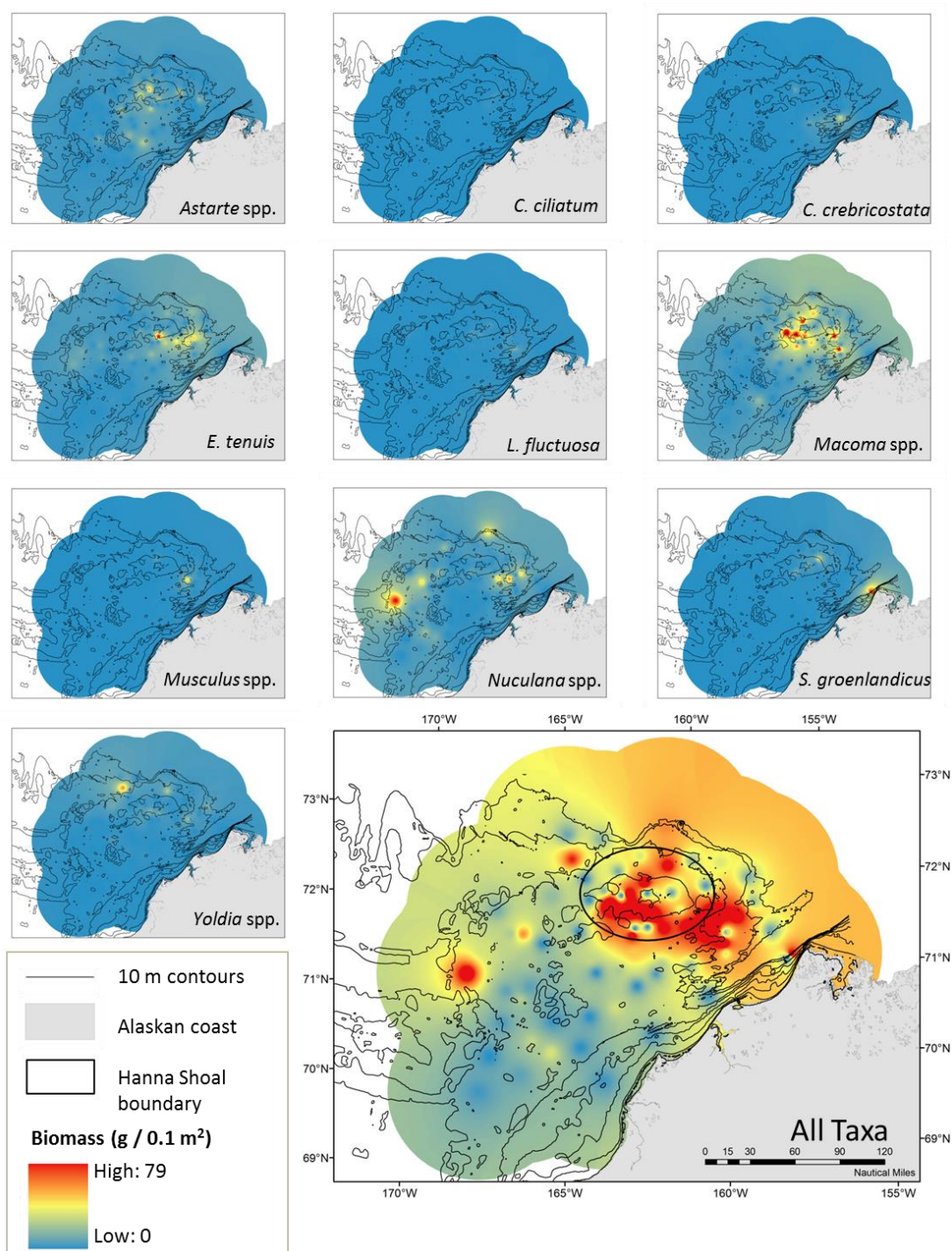


Figure 7: Inverse distance weighting interpolation of biomass (g / 0.1 m²) for each individual taxon and for all taxa combined, clipped to a 60 nautical mile buffer zone surrounding the study region.

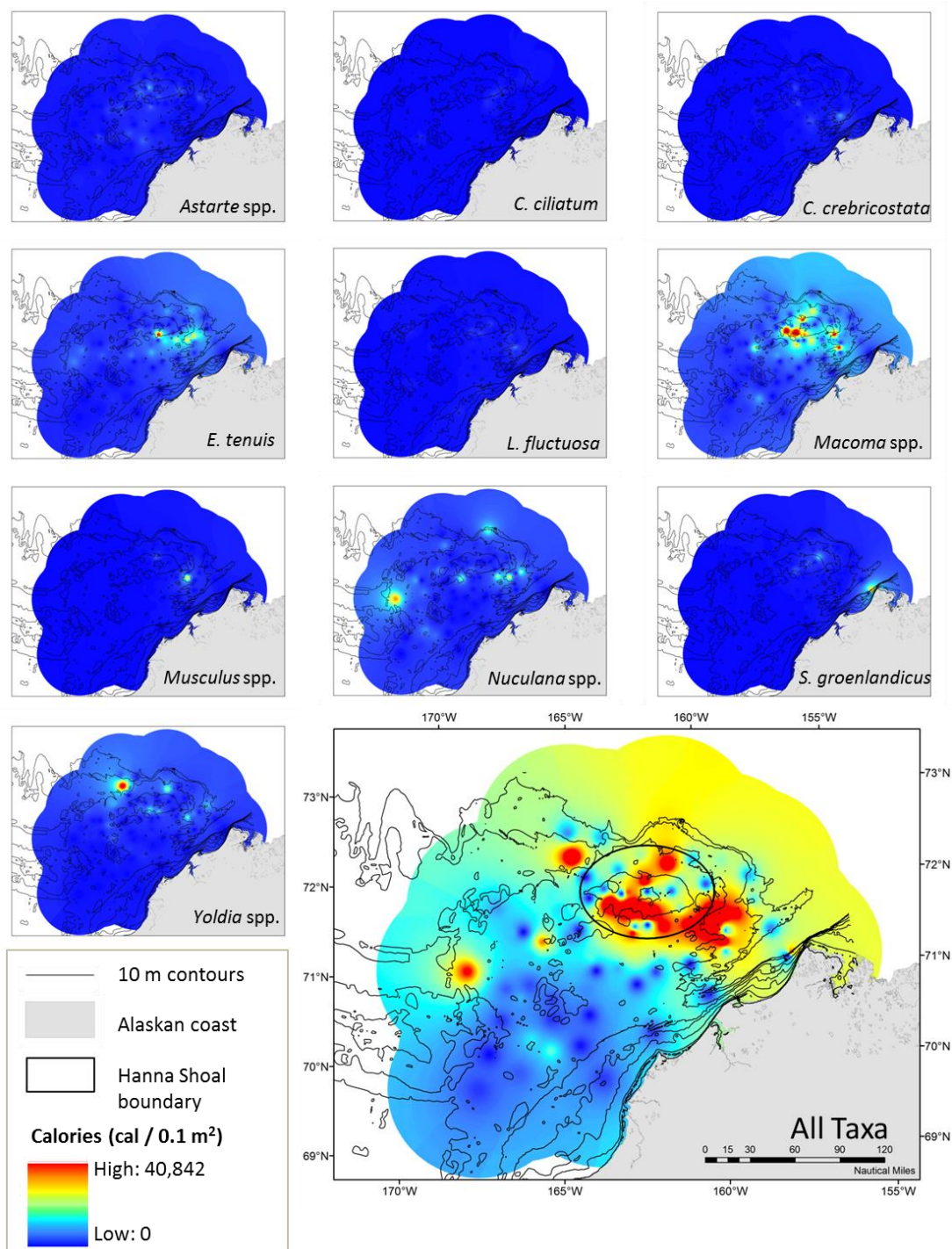


Figure 8: Inverse distance weighting interpolation of caloric distribution (calories / 0.1 m²) for each individual taxon and for all taxa combined, clipped to a 60 nautical mile buffer zone surrounding the study region.

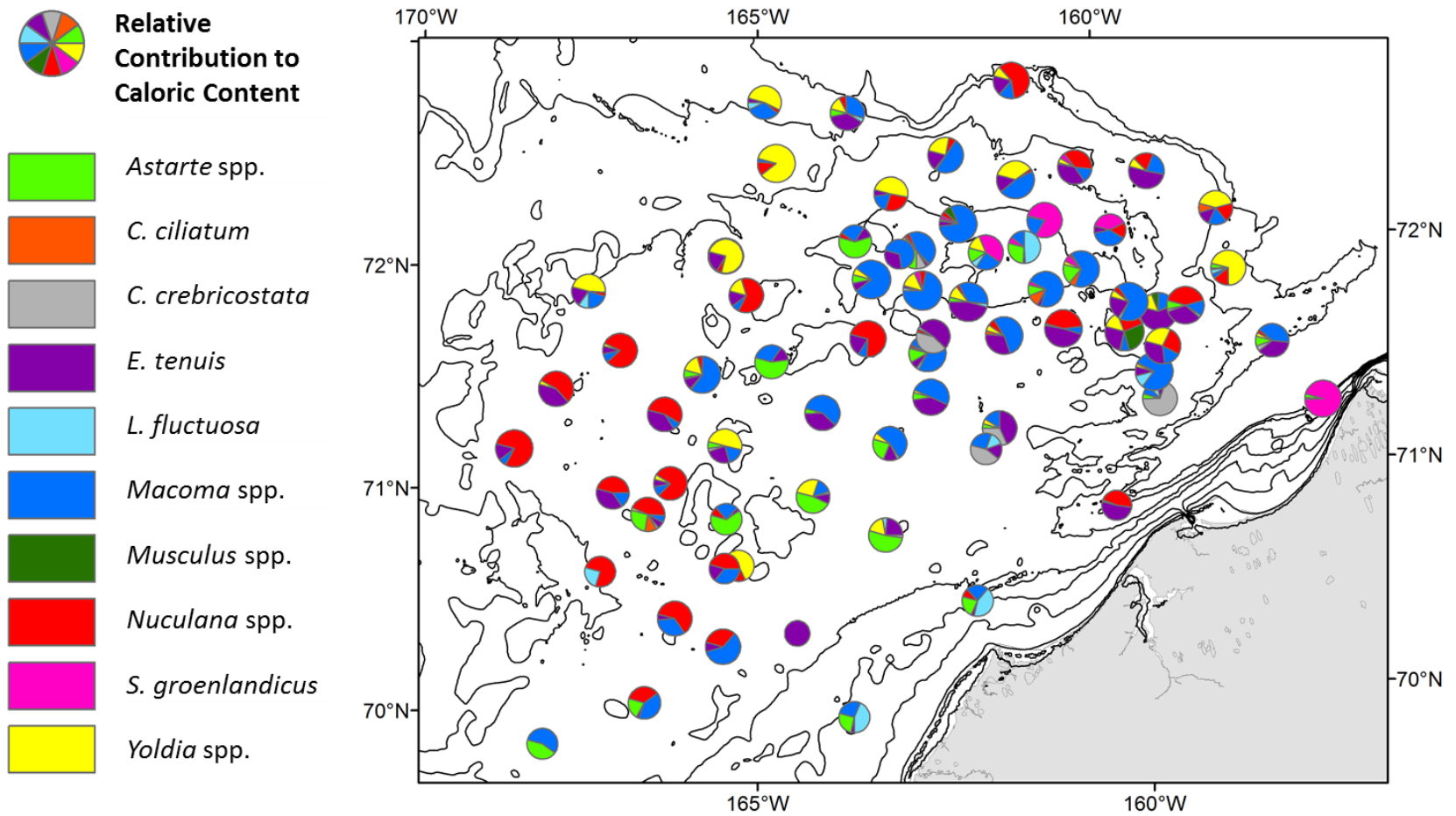


Figure 9: Relative contribution to total caloric content of each station by each taxon. Pie chart size is scaled to log-transformed total caloric content.

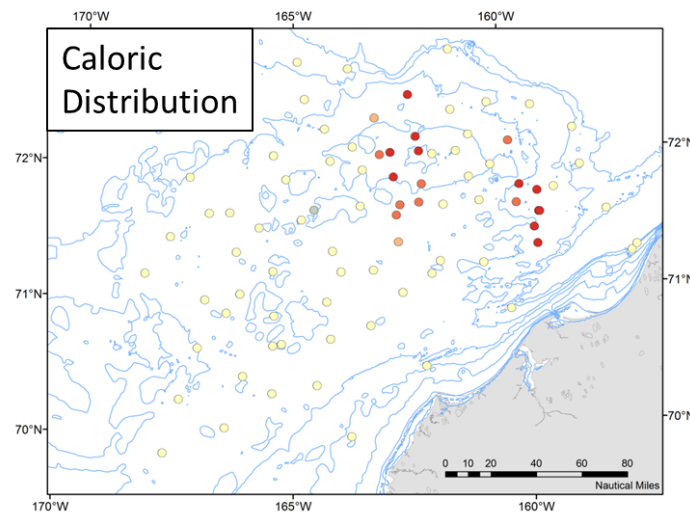
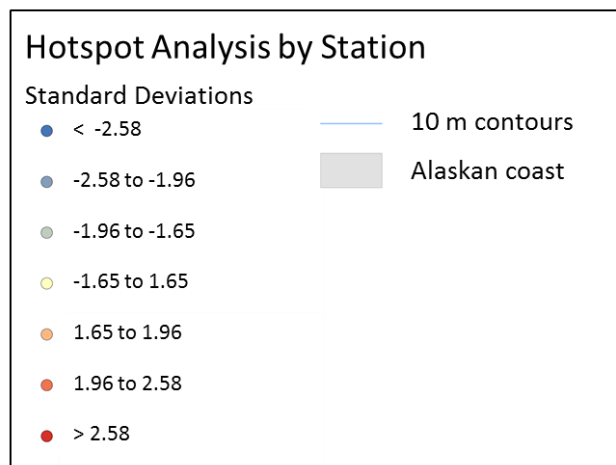
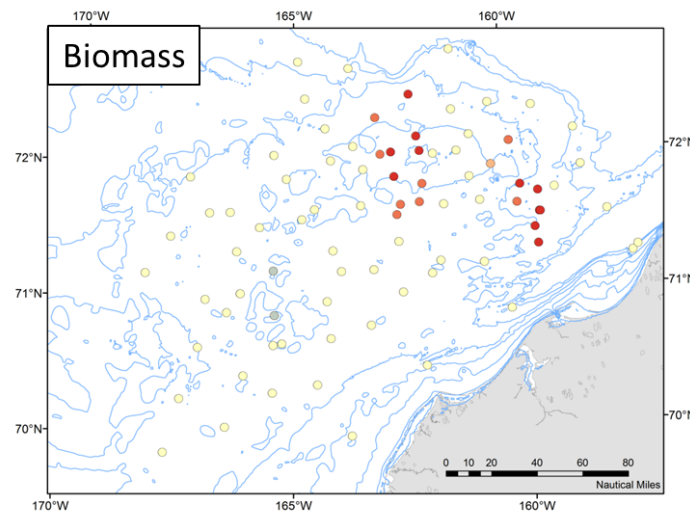
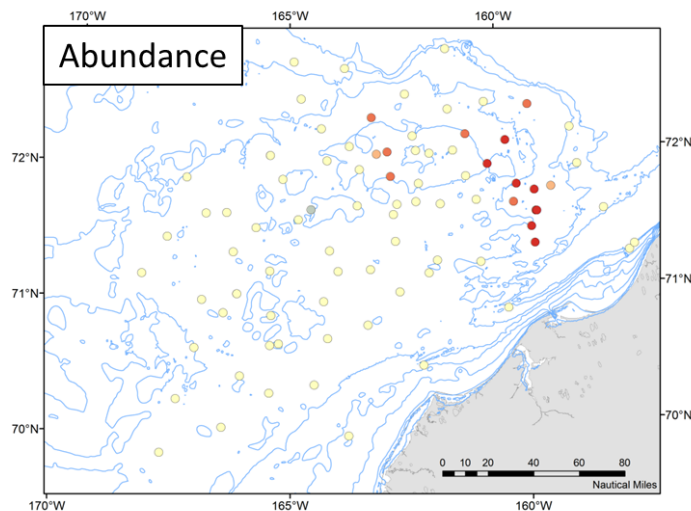


Figure 10: Getis-Ord-GI* hotspot analysis of total mean abundance, biomass and calories by station. Stations with unusually high values (>2.58 standard deviations) are shown in red

Month	Walrus Abundance	F	p-value
June	924	4.276	0.00581*
July	12,654	20.85	1.03e-14*
August	10,280	32.85	<2e-16*
September	2,585	5.944	0.000143*
October	24	0.696	0.405
All Months	26,467	28.48	<2e-16*

Table 5: Pacific walrus abundance by month and results of ANOVA analysis of log-transformed mean caloric value in grid cells with different levels of walrus abundance (n = 0, 1-10, 11-100, 101-1000, and 1001+ walrus per cell). Significant results (p-value < 0.05) are denoted with an asterisk*

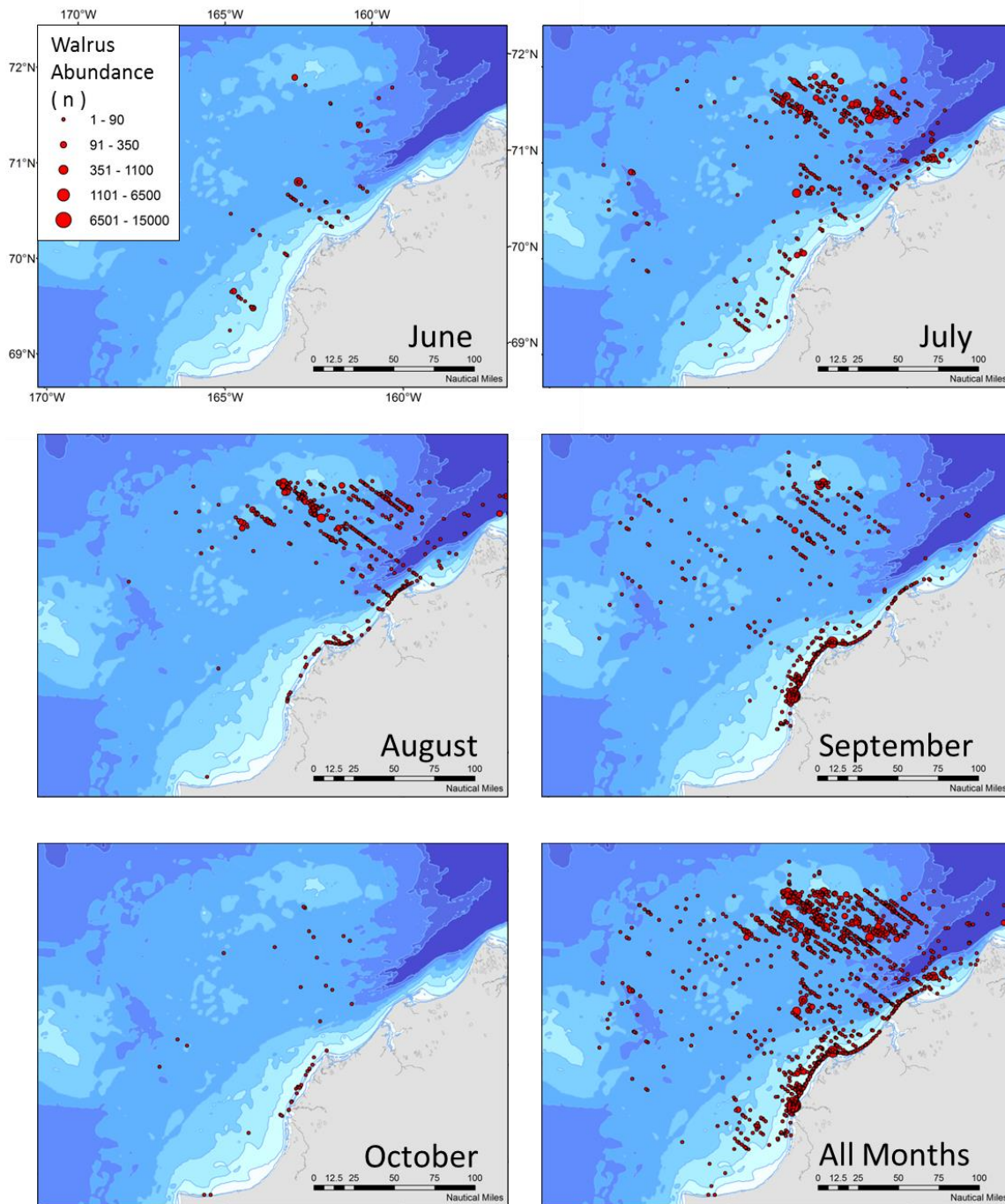


Figure 11: Walrus abundance and distribution in the study area in June, July, August, September, October and all months combined. Data provided by NOAA ASAMM program.

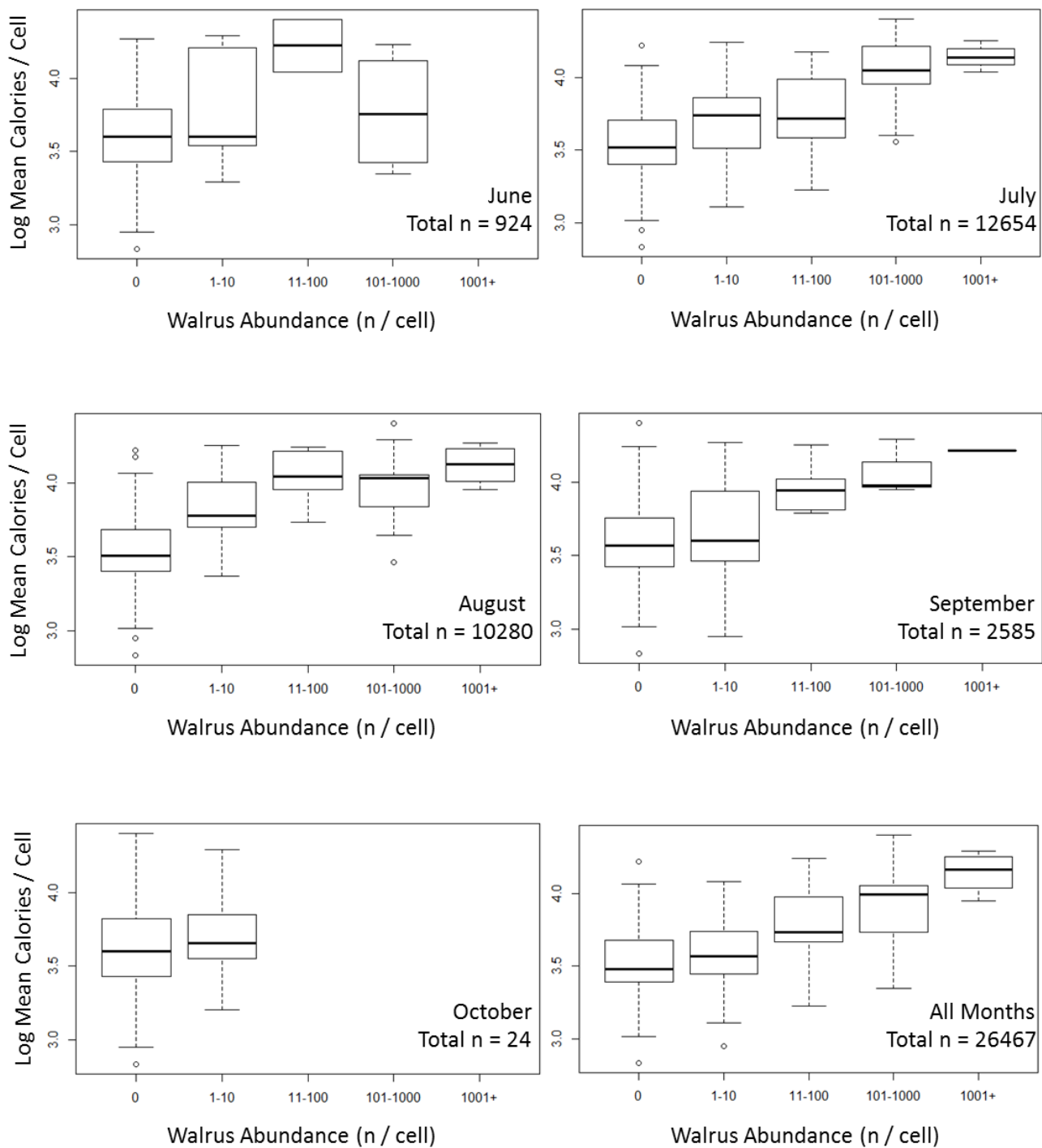


Figure 12: Log-transformed mean calories per cell across various levels of walrus abundance for June, July, August, September, October and all months combined.

DISCUSSION

These results depict a bivalve community that is dominated by a relatively small number of high-calorie taxa. However, the proximate factors responsible for the high caloric density of these taxa are still unknown, as are the environmental factors (such as temperature, sediment grain size, etc.) that might support their dominance over other taxa. These dominant taxa share a distinctive deposit-feeding mode that may confer a competitive advantage over suspension-feeding bivalves in the northeastern Chukchi Sea and contribute to their elevated caloric density, perhaps by facilitating the efficient uptake of select food sources. The current domination of the Hanna Shoal bivalve communities by calorie-dense taxa creates a favorable environment for both vertebrate and invertebrate bivalve predators, as the most common bivalves are those that offer the highest return in terms of calories per gram of tissue consumed. However, the benthic communities of the northeastern Chukchi Sea are likely to be strongly impacted by the effects of climate change on primary productivity regimes, and the distinctive deposit feeding mode of these high-calorie bivalves may make them more vulnerable than the other taxa in our study.

Increased rates of sea ice retreat, along with a decrease in ice algal contributions to the benthos, could enable the replacement of high-calorie bivalve taxa by low-calorie taxa, which could impact higher trophic levels (Richman and Lovvorn 2003, Lovvorn et al. 2003). It is also possible that shifting primary productivity regimes in the region could lead to an overall reduction in export of energy to the benthos, with an associated reduction in abundance and biomass of bivalves and other benthic taxa that would also affect higher trophic levels (Grebmeier et al. 2006a, 2006b). A better understanding of the environmental drivers of these communities and the ways that they respond to changing environmental conditions is particularly important, because climate-driven

shifts in bivalve community composition and overall abundance have been linked to declines in populations of bivalve consumers in other geographic regions.

Shifting environmental conditions may act on these bivalve communities by influencing recruitment rates in the affected populations. Successful recruitment in bivalve populations can be driven by a number of biotic and abiotic factors, including bottom water temperature (Harding et al. 2008), predation (Beukema and Dekker 2014, Dekker and Beukema 2014) and availability of hard substrate for spat recruitment (Skazina et al. 2013). The size-frequency distributions for most taxa examined in this study showed high abundance of specimens in small size classes and decreased abundance at larger size classes. My results are similar to size-frequency distributions reported for Chukchi bivalve taxa living in other geographic areas (Zettler 2002), and may be driven by successful recruitment of spat and juveniles in recent years and/or selective predation pressure on large specimens by bivalve consumers such as Pacific walrus and bearded seals. A few taxa also showed slightly bimodal size frequency distributions, suggesting that at least some taxa may be experiencing fluctuations in recruitment success. However, without annually resolved data and exact specimen ages, it is difficult to speculate on the potential environmental drivers of recruitment success for these taxa. Furthermore, as these bivalves can potentially live for decades, the time span of this study is insufficient to capture long-term variation in recruitment patterns (Strayer and Malcom 2006, Beukema et al. 2010, Skazina et al. 2013). Because instability in population age structure caused by fluctuations in recruitment success are common in many bivalve populations (Gerasimova and Maximovich 2013, Skazina et al. 2013), longer-term studies of population age structure with annual resolution, as well as investigation into the potential environmental drivers of recruitment, are needed before

any conclusions about the stability of the bivalve community in the Hanna Shoal region can be drawn.

Spatial Analysis of Bivalve Abundance, Biomass and Caloric Distribution

The taxa with the highest mean gross heats of combustion (*Yoldia* spp., *Macoma* spp., *Nuculana* spp. and *E. tenuis*) were all deposit feeders. The unusually high caloric density of these taxa may reflect a selective consumption of certain high value foods such as ice algae, which is rich in polyunsaturated fatty acids (PUFAs, Falk-Petersen et al. 1998) and has been shown to be preferentially consumed by deposit feeders (McMahon et al. 2006, Sun et al. 2009). In addition, the reproductive stage of an animal may influence whole animal caloric content in bivalves (Rodriguez et al. 2011) as well as other marine and aquatic organisms (Neves and Brayton 1982, Montevocchi and Piatt 1984, Manhas et al. 2013, Penney and Moffitt 2014). As the reproductive status of bivalves was not examined in this study, it is possible that at the time of sampling these deposit-feeding taxa possessed increased energy reserves as a result of preparation for spawning, while the suspension feeding taxa may have already spawned, resulting in lower overall caloric content for these taxa. An analysis of proximate composition, as well as an in-depth investigation into the reproductive phenology of Chukchi bivalves, might shed some light on the factors driving this significant difference in caloric density among taxa.

Bivalve abundance, biomass and caloric distribution were dominated by high-calorie deposit feeding taxa, and areas of highest bivalve productivity were centered directly on Hanna Shoal and in areas to the south and southeast of the shoal. The high productivity in this area is likely supported by the efficient delivery of nutrients from Pacific-originating waters, particularly BSW, which is thought to play an important role

in the deposition of nutrients and carbon on the shoal and in nearby Barrow Canyon (Weingartner et al. 2005). Furthermore, it has been proposed that Hanna Shoal is the site of convergence of two water masses, as Bering Sea Water (a mixed water mass resulting from the convergence of BSW and AW north of the Bering Strait) circulates around the shoal in a clockwise pattern and draws cold, dense winter-formed water from the northeast into the region. It has been proposed that the clockwise circulation of these water masses around Hanna Shoal may enhance carbon deposition rates, particularly in the region just south of the shoal (Weingartner et al. 2013). This hypothesis has been supported by studies which have measured high salinities and low temperatures typical of northern water masses in bottom waters to the south of the shoal, in conjunction with low C:N ratios (indicative of recent carbon deposits) and high abundance and biomass of benthic infauna (Schonberg et al. 2014).

With regards to the environmental drivers of species dominance among bivalve communities in this region, other studies have examined the influence of environmental parameters on the distribution of epibenthic taxa in the Chukchi Sea and found that parameters such as latitude, longitude, local water masses, depth, temperature, pH, dissolved oxygen, sediment grain size, sediment percent total organic carbon and sediment chlorophyll a can all influence the abundance and distribution of species (Konar et al. 2014, Ravelo et al. 2014). These factors were not examined in this study, but could be a next step in assessing the drivers of the spatially heterogeneous distribution of bivalve taxa observed in this study.

Influence of Bivalve Caloric Distribution on Pacific Walrus Abundance and Distribution in Offshore Feeding Areas

Our findings on the abundance of Pacific walrus in the Hanna Shoal region over the course of the year reflect current knowledge of walrus migration patterns, feeding

habits and habitat use in the Chukchi Sea. In June, Pacific walrus are still en route to the northeastern Chukchi Sea, and I observed correspondingly low walrus abundance in our study area during this month (Fay 1982, Fay et al. 1984). I documented the highest abundance of walrus in our study area during July and August, when the majority of walrus summering on the Alaskan coast are thought to have reached the northeastern Chukchi Sea (Fay 1982), and when walrus foraging around Hanna Shoal is thought to be most intense (Jay et al. 2012).

Historically, walrus remain in offshore foraging areas such those around Hanna Shoal through the remainder of summer and into the early fall (Fay 1982, Fay et al. 1984), but recent reductions in sea ice extent and duration have made it more difficult for walrus to spend significant amounts of time foraging in offshore areas in September, when sea ice reaches its minimum extent (Stroeve et al. 2012). Walrus require sea ice to serve as a platform for hauling out and resting between feeding bouts in offshore areas (Fay 1982), and because sea ice extent has reached all-time historical lows in recent years (Stroeve et al. 2012, Wang and Overland 2012), walrus are increasingly hauling out on the Alaskan coast in late summer and early fall (Jay et al. 2012). This may explain the reduced abundance of walrus observed in the offshore study area in September. However, despite this reduced abundance, I still observed a significant correlation between high bivalve caloric density and high densities of walrus, which I believe indicates continued foraging around Hanna Shoal in September despite low sea ice extent in these years. Others have documented large numbers of radio-tagged walruses traveling from coastal haulout locations to the foraging grounds of Hanna Shoal, completing a round trip of over 200 km (Jay et al. 2012). This massive expenditure of energy highlights the importance of the Hanna Shoal region as a high-value foraging ground for Pacific walrus, even in low ice years. After September, very few walrus remained in the study area, likely due to

the onset of the southern migration with the rapid formation of new sea ice in October (Fay 1982). This could also be due to movements of walrus from the coast of Alaska to the coast of Chukotka in Russia, where sea ice tends to persist longer and allows walrus to remain in offshore foraging locations longer than in the northeastern Chukchi Sea (Jay et al. 2012).

This study focused exclusively on bivalves, as they are a preferred food resource for Pacific walrus that are also consumed by other walrus prey items, most notably gastropods. However, walrus feeding in the Chukchi also consume prey items that are not bivalve consumers, such as polychaete worms (Fay 1982, Sheffield and Grebmeier 2009). As such, a truly comprehensive predictive model of walrus abundance and distribution in foraging areas should incorporate the distribution of all benthic taxa from walrus prey guilds, as well as availability of haulout platforms in the region, whether they be coastal or sea ice. However, despite the potential confounding influence of sea ice on walrus abundance and distribution in the study area and the exclusion of other prey taxa, I still found a significant correlation between bivalve caloric distribution and abundance and distribution of Pacific walrus in the study area.

Implications of Global Change

The reduction of sea ice extent and duration could have a bottom-up impact on the bivalve communities of Hanna Shoal through altering the dynamics of primary productivity in the Chukchi Sea. For example, as a result of shifting sea ice dynamics, the relative contributions of ice algae and phytoplankton to benthic communities are likely to change. Diatom-dominated, PUFA-enriched ice algae represents one of the first sources of high quality food available to benthic communities after the winter (Falk-Petersen et al. 1998, Arrigo and Thomas 2004, Sun et al. 2009), and is readily assimilated by benthic

fauna (Yunker et al. 1995, Macdonald et al. 1998, Mincks et al. 2005, Ratkova and Wassmann 2005, McMahon et al. 2006, Sun et al. 2007, Renaud et al. 2007, Boetius et al. 2013). High quality foods, and particularly foods that are high in PUFAs, have been shown to enhance reproductive success, larval survival, recruitment and growth in bivalves (Wacker and Elert 2004, Basen et al. 2011), and feeding experiments conducted by McMahon et al. (2006) and Sun et al. (2009) have shown that deposit feeding bivalves may preferentially consume ice algae over other food sources. In our study, the four dominant taxa in terms of abundance, biomass and caloric distribution were all deposit or mixed deposit and suspension feeders, while all other taxa examined are classified as suspension feeders (Macdonald et al. 2010). It is possible that deposit feeding may confer a competitive edge to bivalves in this ecosystem by facilitating the consumption of high-quality food such as ice algae.

Ice algae are dependent on sea ice for substrate and cannot form blooms in open water, making them vulnerable to reductions in sea ice extent and duration (Hegseth 1998, Wassmann et al. 2011). If current trends in reduced sea ice extent and duration continue, the associated loss of substrate for ice algae communities is expected to reduce their relative contribution of organic matter to the benthos (Horner and Schrader 1982, Hsiao 1992, Carroll and Carroll 2003, Arrigo et al. 2008, Arrigo and van Dijken 2011), though this effect has not yet been quantitatively confirmed in the field (Wassmann et al. 2011). If this is the case, it is possible that bivalves from alternative feeding guilds that do not preferentially consume ice algae may gain a competitive edge over the currently dominant deposit feeders in the Hanna Shoal region. In addition, reductions in sea ice algal production could differentially impact members of deposit feeding guilds that utilize different deposit-feeding strategies. For example, it has been proposed that under conditions of reduced ice algal production, deposit feeders that are able to access food

sources buried in the sediment, such as members of the genus *Nuculana*, may gain a competitive advantage over deposit feeders that prefer to feed on surface sediments, such as members of the genus *Macoma* (Weems et al. 2012). The wide variety of feeding strategies employed by Chukchi bivalves must be considered when attempting to predict the impacts of reduced ice algal production on these organisms.

Additional challenges for benthic organisms could arise if altered sea ice dynamics lead to mismatches in the timing of algal blooms with reproductive cycles for benthic organisms. Altered timing of sea ice retreat in recent years has been shown to alter open water phytoplankton community structure in the Chukchi (Fujiwara et al. 2014). In addition, mean snow depth on Chukchi sea ice has declined in recent years (Webster et al. 2014), and reduction of the reflective snow cover on sea ice may result in earlier sea ice retreat and ice algae blooms (Wassmann and Reigstad 2011). Some studies have indicated that the reproductive cycles of arctic grazers such as the copepod *Calanus glacialis* are timed to take advantage of the high quality food available during ice algae blooms (Søreide et al. 2010), and that mismatches in the timing of primary production and copepod reproduction can severely reduce copepod recruitment and abundance (Leu et al. 2011). It is possible that Chukchi bivalves may also time their reproductive events to take advantage of exports of high quality ice algae to the benthos. This hypothesis is supported by studies that found that reproduction was triggered by inputs of high-quality food in the bivalve *Yoldia hyperborea* in Conception Bay, Newfoundland (Stead and Thompson 2003, Jaramillo and Thompson 2008). As such, there could be negative repercussions for these bivalve taxa if altered sea ice dynamics leads to altered timing in ice algal blooms.

Benthic microalgae, or microphytobenthos, are an additional food source for Chukchi bivalves that may be affected by changing sea ice dynamics. Benthic microalgae

are an important component of benthic food webs in shallow marine ecosystems, particularly for deposit and suspension feeders (Miller et al. 1996). Early studies of benthic microalgae in the Chukchi Sea reported extremely high levels of microphytobenthic primary productivity, particularly in August, when rates of carbon fixation (approaching $57 \text{ mg C m}^{-2} \text{ h}^{-1}$) were eight times higher than ice algae productivity and twice as high as pelagic phytoplankton productivity (Matheke and Horner 1974). There is increasing evidence suggesting that the Chukchi could support a viable microphytobenthic community, and that such communities may contribute substantially to benthic primary production in Arctic ecosystems and may exceed pelagic primary productivity by a factor of 1.5, particularly in areas less than 30 m deep such as certain parts of Hanna Shoal (Rysgaard and Nielsen 2006, Glud et al. 2009, McTigue et al. 2015). However, it is uncertain how climate change and alterations in sea ice dynamics might affect microphytobenthic communities in the northeastern Chukchi Sea. Though primary production in the Arctic is expected to increase as higher temperatures reduce sea ice extent and duration and increase available light for photosynthesis (Sakshaug 2004), one study which modeled the effects of a 2°C temperature increase on Arctic microphytobenthic communities predicted only marginal effects on microphytobenthic net community production (Woelfel et al. 2014). A decrease in sea ice coverage will increase the light available for photosynthesis for benthic microalgae, which can fuel their growth by taking up nutrients from bottom waters and sediment porewater (Glud et al. 2009). On the other hand, pelagic phytoplankton, which are more nutrient-limited than benthic microalgae due to their position in the water column, may be better situated to take advantage of the increase in light availability (Glud et al. 2009, Woelfel et al. 2014). Nutrient availability has been shown to influence the balance of

pelagic and benthic production (Glud et al. 2009), and as such, predicting how climate change will impact Arctic primary production is not always straightforward.

Shifts in the abundance and distribution of bivalves have the potential to greatly impact populations of upper trophic level consumers through bottom-up processes. This has been documented in the Wadden Sea, where bivalves are an important source of food for eiders (*Somateria mollissima*), oystercatchers (*Haematopus ostralegus*), and red knots (*Calidris canutus*). A combination of recruitment failure and increased mortality rates in several dominant bivalve species in the Wadden Sea (*Cerastoderma edule*, *Macoma balthica*, and *Mytilus edulis*) caused substantial declines in bird-accessible bivalve biomass and is believed to have contributed to fluctuations in stocks of shellfish-eating birds (Beukema et al. 2010). It is hypothesized that elevated winter temperatures in the Wadden Sea was the main factor that contributed to recruitment failure and increased bivalve mortality, particularly for *M. balthica*, which experiences increased predation pressure on early life stages from the shrimp *Crangon crangon* in warmer years (Beukema and Dekker 2005, 2014, Beukema et al. 2009, 2010, Dekker and Beukema 2014). This example illustrates the dramatic impact that shifts in bivalve communities can have on upper trophic levels, and underscore the importance of understanding how environmental factors drive bivalve population dynamics. In order to predict the effects of changing environmental conditions on upper trophic level consumers such as Pacific walrus, it is critical to first determine the effects these changing conditions will have on the lower trophic levels that support them.

CONCLUSION

Climate change is expected to dramatically alter ecosystem dynamics in the Chukchi Sea, but exactly what form these changes will take is difficult to predict. However, past variability in climate and associated ecosystem responses may provide some insight into how a warming climate will impact this predominantly benthic ecosystem. The Bering Sea provides a poignant example of how a warming regime can affect an ecosystem where primary productivity is controlled by sea ice duration and extent, and how altered sea ice dynamics can impact benthic communities and upper trophic level benthic predators. It is widely accepted that the Bering Sea experienced a major regime shift to warmer conditions in 1976-77, and again to a lesser degree in 1989 (Hare and Mantua 2000, Bond and Adams 2002), with widespread effects on Bering Sea food web dynamics and significant consequences for many upper trophic level consumers, including the threatened spectacled eider (*Somateria fischeri*), a diving duck that winters in an area southwest of St. Lawrence Island where it feeds extensively on bivalves.

The spectacled eider was likely affected by shifts in the bivalve community composition of the northern Bering Sea when the comparatively calorie-rich and formerly dominant *Macoma calcaria* was replaced by the comparatively calorie-poor *Nuculana radiata* as the dominant species by the late 1980's (Sirenko and Koltun 1992, National Research Council 1996, Richman and Lovvorn 2003). Combined with a decline in mean bivalve size and biomass per unit area (Grebmeier and Dunton 2000), this reduction in overall caloric resources may have contributed to declines in the spectacled eider (Richman and Lovvorn 2003, Lovvorn et al. 2003). Though the exact mechanism for this shift in species dominance is not conclusively known, the Bering Sea regime shift to

warmer temperatures is considered likely to have contributed to the shift in bivalve species dominance (National Research Council 1996, Richman and Lovvorn 2003). In my study, high-calorie deposit-feeding bivalve taxa tended to dominate measures of numerical abundance, biomass and caloric distribution. As such, shifts in community composition could significantly impact the available caloric resources for bivalve predator populations in the Chukchi Sea, especially if these high caloric density taxa were to be supplanted by low caloric density taxa.

The driving mechanism of change in the Bering Sea may have been sea ice, which directs the bulk of Bering Sea primary production into either benthic or pelagic pathways depending on the timing of sea ice retreat and the spring bloom (Hunt et al. 2002). In colder years, sea ice persists late into the year, and early primary productivity occurs as an ice-edge associated bloom in cold waters that thermally limit zooplankton grazing, resulting in large amounts of carbon sinking to the benthos and promoting benthic-pelagic coupling. In warmer years, early sea ice recession delays large blooms of primary production until cessation of storm activity and thermal stratification stabilizes the water column, resulting in an open-water bloom with high levels of zooplankton grazing, and diverting large amounts of productivity away from the benthos and into pelagic food webs (Hunt et al. 2002). Others have proposed that altered sea ice dynamics could have similar repercussions on food webs in the Chukchi Sea, and that reductions in sea ice duration and extent may shift the region from a benthic-dominated ecosystem to a pelagic-dominated ecosystem (Grebmeier et al. 2006a), affecting recruitment success and stability of Chukchi bivalve populations. If altered sea ice dynamics in the Chukchi result in the bulk of primary production being shifted into pelagic food webs, this would result in dramatic impacts on the benthic communities of the region and the benthic feeding apex consumers that depend on them.

Appendices

APPENDIX A

Effects of Preservation on Length-Weight Ratio

Each taxon that showed a significant difference in log-transformed length-weight ratio between years was analyzed with additional ANCOVA comparisons of log-transformed length-weight ratios of each year of preservation with those of frozen specimens. Specimens were assigned a preservation year class based on how many years they had been chemically preserved at the time of analysis. Year Zero represented frozen specimens, Year One represented specimens collected in 2013, Year Two represented specimens collected in 2012, Year Four represented specimens collected in 2010, and Year Five represented specimens collected in 2009.

The results of the pairwise ANCOVA analyses were variable and differed by taxa. All year classes of *Astarte* spp. and *L. fluctuosa* showed significant differences in length-weight ratios from Year Zero except Year Five. Years One and Two of *C. crebricostata* showed significant differences from Year Zero, but not Years Four or Five. The remaining taxa showed only one significantly different year class, with Year One being significantly different for *E. tenuis*, Year Four being significantly different for *Musculus* spp., and Year Five being significantly different for *Nuculana* spp. (Table A1).

To further examine the effects of these differences on the predicted weights of specimens of these taxa, weights for standard lengths were predicted for each year class and compared to Year Zero. This was done using the slope and y-intercept parameters of the regressions of the natural logs of length and weight for each taxon, and weights were predicted for lengths of 5-40 mm in increments of 5 mm (Figure A1).

Three year classes of *Astarte* spp. (Years One, Two and Four) showed significant differences from Year Zero, and the predicted weights for standard sizes showed that all preserved year classes had lower weights than Year Zero specimens of the same size (Figure A1). However, there was no clear pattern of weight loss, with Years Four and Two having the lightest predicted weights, followed closely by Year One. Year Five specimens were predicted to have a significantly heavier weight than all other preserved years, and the length-weight ratios from this preservation year were not significantly different from Year Zero. If chemical preservation were affecting specimen weights, I would expect to see a uniform weight loss across all years, or a loss of weight that increased with increasing preservation time, as alcohol-preserved specimens do not typically gain weight while preserved (Mills et al. 1982, Shields and Carlson 1996, Qureshi et al. 2008, Melo et al. 2010). In addition, any weight fluctuations that occur as a result of chemical preservation tend to stabilize within one month to four months of preservation (Mills et al. 1982, Shields and Carlson 1996, Qureshi et al. 2008, Melo et al. 2010). As such, an increase in specimen weight after five years of preservation as seen in *Astarte* spp. is unlikely.

Two year classes of *C. crebricostata* (Years One and Two) showed significantly different length-weight ratios than Year Zero specimens (Figure A1). However, for these years, the projected weights were actually higher than those of frozen specimens. Similarly, three year classes of *L. fluctuosa* (Years One, Two and Four, Figure A1) and one year class of *Musculus* spp. (Year Four, Figure A1) showed significant differences from Year Zero, but all significantly different years were projected to have higher weights at standard lengths than any frozen specimens. As weight gain is not a typical feature of alcohol preservation, I consider this to be weak evidence of a preservation effect on weight.

One year class of *E. tenuis* (Year One, Figure A1) and one year class of *Nuculana* spp. (Year Five, Figure A1) showed a significantly different length-weight ratio from Year Zero specimens, and the projected weights for these year classes were lighter than those of frozen specimens. This could be considered evidence of a potential preservation effect, although weight loss due to chemical preservation has typically stabilized before a full year of preservation has passed, making changes in length-weight ratios after one or five years of preservation somewhat unlikely. In addition, as these are the only taxa which show this potential effect, and they display opposite patterns in terms of the timing of the effect (changes in length-weight ratios after the first year of preservation vs. after the fifth year), it is possible that this could be due to some other source of variation.

One possible alternative source of variation in the length-weight ratios of the taxa discussed here include random variation in the length-weight ratios of the specimens collected within a particular year. Specimens of *Astarte* spp., *Musculus* spp. and *Nuculana* spp. were only identified to the genus level, and it is possible that subtle differences in shell morphometrics of different species within these taxa could contribute to different length-weight ratios, particularly if one species was more abundant in certain years than in others. In the case of *C. crebricostata*, it is possible that varying levels of erosion of the unusually thick periostracum of this species could have contributed to variation in length-weight ratios between years. In addition, a bivalve's rates of growth of linear shell length and shell thickness can vary depending on environmental cues; for example, one species of mussel has been found to increase shell thickness at the expense of linear shell growth when raised in the presence of chemical cues from predators such as whelks, crabs and sea stars (Smith and Jennings 2000), which would produce variation in the length-weight ratio. Furthermore, soft tissue weight can constitute a significant portion of the wet weight of an animal, and variations in soft tissue weight could also

alter length-weight ratios. For example, Lewis and Cerrato (1997) demonstrated that minimal feeding resulted in loss of soft tissue weight in bivalves over a period of just a few weeks, so it is possible that variations in food availability could lead to interannual variation in length-weight ratio if food resources were scarce in the weeks prior to sampling.

Overall, these results do not show a clear effect of preservation on the weights of the specimens in this study. If an effect were present, I would not expect it to affect some taxa and not others, as I saw here. In addition, if an effect of preservation were present, I would expect to see a consistent pattern across years, rather than the variable differences between years that were observed in the six taxa which had at least one significantly different year. It should be noted that the specimens included in this study were preserved for relatively short periods of time (1-5 years) compared to some historical benthic invertebrate collections, so it is possible that longer preservation times could affect length-weight ratios. However, for this study, it seems more likely that some other factor is responsible for the observed differences in length-weight ratios observed in these taxa, and with no clear pattern of weight loss or gain across taxa and preservation years, I feel that the application of a correction factor is unjustified.

Taxon	Year One : Year Zero	Year Two : Year Zero	Year Four : Year Zero	Year Five: Year Zero
<i>Astarte</i> spp.	< 0.001*	0.005147*	< 0.001*	0.64140
<i>C. crebricostata</i>	< 0.001*	0.001895*	0.3892	0.1427
<i>E. tenuis</i>	0.01881*	0.465	0.11850	0.1905122
<i>L. fluctuosa</i>	< 0.001*	< 0.001*	< 0.001*	0.3287
<i>Musculus</i> spp.	0.6288	0.26808	0.00284*	n/a
<i>Nuculana</i> spp.	0.7987	0.8563053	0.8111586	< 0.001*

Table A1: Results of multiple regressions of taxa with statistically significant differences in log-transformed length-weight ratios between years. Log-transformed length-weight ratios of each year of preservation were compared to log-transformed length-weight ratio of frozen bivalves (Year Zero) to identify significantly different years. Note that no specimens of *Musculus* spp. were collected in 2009, so no Year Five comparison was possible. Significant results (p-value < 0.05) are shown with an asterisk*.

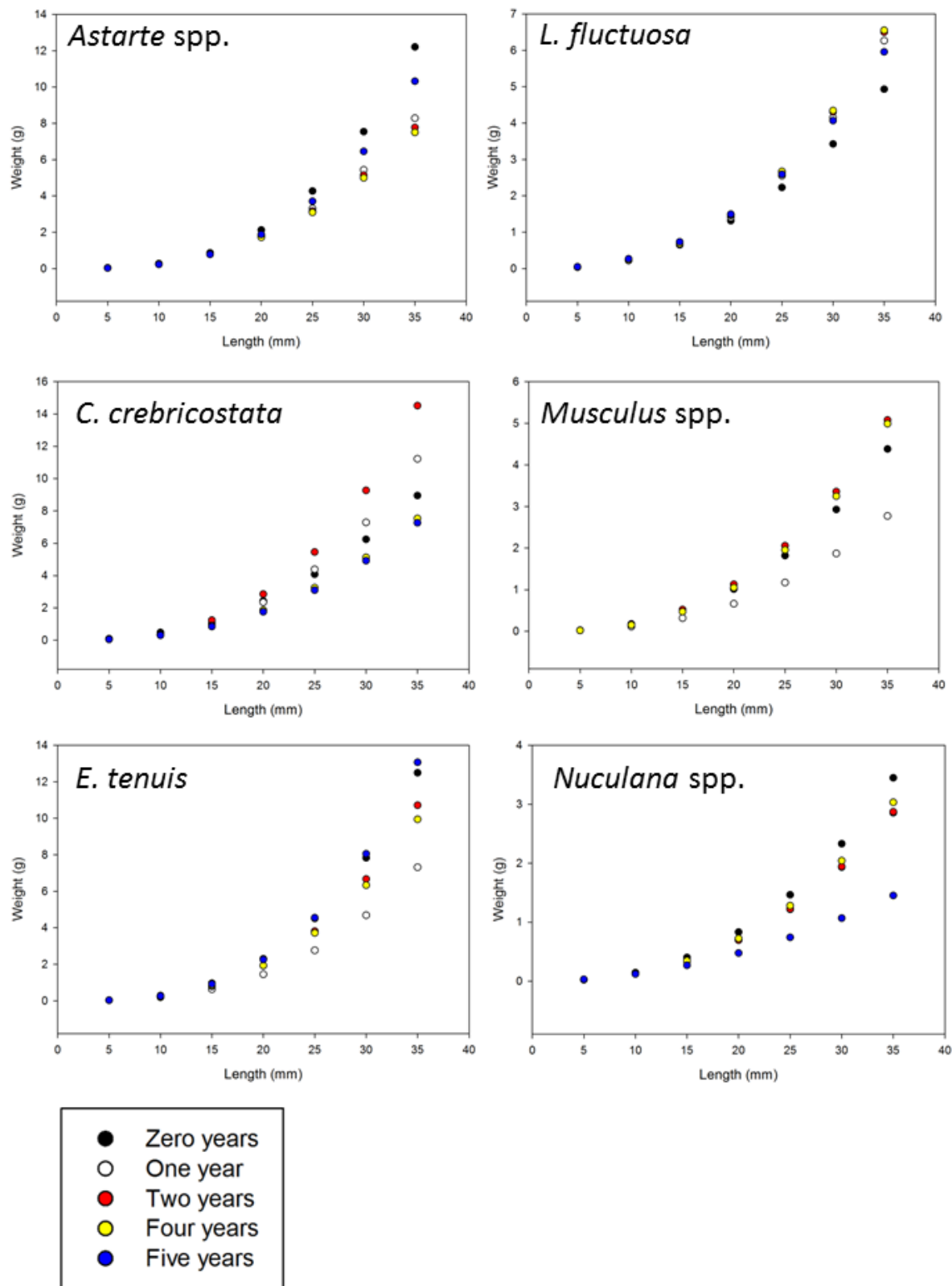


Figure A1: Projected weights of standard lengths across all years of preservation.

APPENDIX B

	Inverse Distance Weighting	Completely Randomized Spline	Spline with Tension	Ordinary Kriging	Empirical Bayesian Kriging
<i>Astarte</i> spp.	1.520692	1.383483	1.382707	1.362111	1.385533
<i>C. ciliatum</i>	0.19743	0.196905	0.196901	0.208781	0.198715
<i>C. crebricostata</i>	0.975077	0.930152	0.930165	0.950766	0.923554
<i>E. tenuis</i>	19.46012	19.31353	19.27312	19.57665	20.23609
<i>L. fluctuosa</i>	0.707402	0.677717	0.678111	0.713453	0.696617
<i>Macoma</i> spp.	14.68220563	14.68220563	14.68220563	14.68220563	14.68220563
<i>Musculus</i> spp.	0.569411	0.555971	0.555975	0.554286	0.563771
<i>Nuculana</i> spp.	9.527368	9.243455	9.174616	8.476792	8.375378
<i>S. groenlandicus</i>	0.442509958	0.442509958	0.442509958	0.442509958	0.442509958
<i>Yoldia</i> spp.	7.735141	7.598938	7.59896	7.632071	7.644552
All Taxa	36.88717	36.39647	36.34465	36.61316	37.27443

Table B1: Root mean squared errors of cross-validation comparison of interpolation techniques for abundance.

	Inverse Distance Weighting	Completely Randomized Spline	Spline with Tension	Ordinary Kriging	Empirical Bayesian Kriging
<i>Astarte</i> spp.	0.198351	0.180454	0.180353	0.177667	0.180722
<i>C. ciliatum</i>	0.118458	0.118143	0.118141	0.125269	0.119229
<i>C. crebricostata</i>	0.177287	0.169119	0.169121	0.172867	0.167919
<i>E. tenuis</i>	0.143089	0.142011	0.141714	0.143946	0.148795
<i>L. fluctuosa</i>	0.163247	0.156396	0.156487	0.164643	0.160758
<i>Macoma</i> spp.	0.176894	0.172293	0.172291	0.170268	0.174325
<i>Musculus</i> spp.	0.142353	0.138993	0.138994	0.138571	0.140943
<i>Nuculana</i> spp.	0.210163	0.2039	0.202381	0.186988	0.184751
<i>S. groenlandicus</i>	0.147503	0.132712	0.132401	0.13573	0.130519
<i>Yoldia</i> spp.	0.143243	0.140721	0.140721	0.141335	0.141566
All Taxa	0.200838	0.198166	0.197884	0.199346	0.202946

Table B2: Normalized root mean squared errors of cross-validation comparison of interpolation techniques for abundance.

	Inverse Distance Weighting	Completely Randomized Spline	Spline with Tension	Ordinary Kriging	Empirical Bayesian Kriging
<i>Astarte</i> spp.	4.040851	3.651045	3.6421	3.656957	3.573468
<i>C. ciliatum</i>	0.196913	0.19583	0.195909	0.189977	0.198025
<i>C. crebricostata</i>	1.399261	1.36805	1.368106	1.375225	1.361512
<i>E. tenuis</i>	4.827054	4.787358	4.782248	4.883781	4.976793
<i>L. fluctuosa</i>	0.819309	0.787634	0.788019	0.818758	0.817154
<i>Macoma</i> spp.	10.20866	9.740869	9.732128	9.982718	9.614408
<i>Musculus</i> spp.	2.118915	2.082863	2.082888	2.074331	2.124161
<i>Nuculana</i> spp.	5.555183	5.588512	5.585813	5.728097	5.537245
<i>S. groenlandicus</i>	5.390676	4.309129	4.289856	4.189738	4.167541
<i>Yoldia</i> spp.	3.019905	2.974153	2.970855	3.029861	2.933269
All Taxa	18.29628	17.33116	17.33133	17.68767	17.18581

Table B3: Root mean squared errors of cross-validation comparison of interpolation techniques for biomass.

	Inverse Distance Weighting	Completely Randomized Spline	Spline with Tension	Ordinary Kriging	Empirical Bayesian Kriging
<i>Astarte</i> spp.	0.172318	0.155695	0.155314	0.155947	0.152387
<i>C. ciliatum</i>	0.160287	0.159406	0.15947	0.154641	0.161193
<i>C. crebricostata</i>	0.127886	0.125034	0.125039	0.125689	0.124436
<i>E. tenuis</i>	0.140698	0.139541	0.139392	0.142352	0.145063
<i>L. fluctuosa</i>	0.131773	0.126678	0.12674	0.131684	0.131426
<i>Macoma</i> spp.	0.202042	0.192784	0.192611	0.19757	0.190281
<i>Musculus</i> spp.	0.114383	0.112437	0.112439	0.111977	0.114667
<i>Nuculana</i> spp.	0.177575	0.17864	0.178554	0.183102	0.177001
<i>S. groenlandicus</i>	0.155793	0.124536	0.123979	0.121085	0.120444
<i>Yoldia</i> spp.	0.132681	0.130671	0.130526	0.133118	0.128874
All Taxa	0.231325	0.219122	0.219124	0.22363	0.217285

Table B4: Normalized root mean squared errors of cross-validation comparison of interpolation techniques for biomass.

	Inverse Distance Weighting	Completely Randomized Spline	Spline with Tension	Ordinary Kriging	Empirical Bayesian Kriging
<i>Astarte</i> spp.	732.4595	665.4486	664.0569	665.1807	656.0309
<i>C. ciliatum</i>	109.6763	109.0734	109.1175	105.8131	110.2961
<i>C. crebricostata</i>	440.9751	426.6969	426.1488	443.1821	422.9838
<i>E. tenuis</i>	2457.329	2436.629	2435.177	2475.007	2522.6
<i>L. fluctuosa</i>	320.529	308.2645	308.4558	320.7862	320.7481
<i>Macoma</i> spp.	5383.011	5175.758	5171.365	5324.568	5112.9
<i>Musculus</i> spp.	1233.209	1212.226	1212.241	1207.261	1236.262
<i>Nuculana</i> spp.	2246.083	2254.118	2253.091	2276.167	2240.893
<i>S. groenlandicus</i>	1931.633	1544.283	1537.408	1505.691	1492.069
<i>Yoldia</i> spp.	2531.388	2489.174	2486.217	2540.68	2451.6
All Taxa	8864	8606.43	8608.282	8733.056	8664.253

Table B5: Root mean squared errors of cross-validation comparison of interpolation techniques for calories.

	Inverse Distance Weighting	Completely Randomized Spline	Spline with Tension	Ordinary Kriging	Empirical Bayesian Kriging
<i>Astarte</i> spp.	0.182805	0.166081	0.165734	0.166014	0.163731
<i>C. ciliatum</i>	0.160287	0.159406	0.15947	0.154641	0.161193
<i>C. crebricostata</i>	0.141285	0.136711	0.136535	0.141992	0.135521
<i>E. tenuis</i>	0.140425	0.139242	0.139159	0.141435	0.144155
<i>L. fluctuosa</i>	0.13186	0.126814	0.126893	0.131966	0.13195
<i>Macoma</i> spp.	0.184428	0.177327	0.177177	0.182425	0.175173
<i>Musculus</i> spp.	0.114383	0.112437	0.112439	0.111977	0.114667
<i>Nuculana</i> spp.	0.183178	0.183833	0.183749	0.185631	0.182755
<i>S. groenlandicus</i>	0.155835	0.124586	0.124031	0.121472	0.120373
<i>Yoldia</i> spp.	0.13291	0.130693	0.130538	0.133398	0.128721
All Taxa	0.216935	0.210632	0.210677	0.213731	0.212047

Table B6: Normalized root mean squared errors of cross-validation comparison of interpolation techniques for calories.

	10	20	30	40	50
<i>Astarte</i> spp.	1.539156	1.51261	1.491356	1.485809	1.479701
<i>C. ciliatum</i>	0.197513	0.197	0.19693	0.19682	0.196826
<i>C. crebricostata</i>	0.981449	0.966216	0.963553	0.962041	0.962807
<i>E. tenuis</i>	19.68533	19.37945	19.33149	19.25154	19.23096
<i>L. fluctuosa</i>	0.710726	0.702071	0.698254	0.694929	0.69153
<i>Macoma</i> spp.	14.71304	14.65464	14.67239	14.66474	14.66005
<i>Musculus</i> spp.	0.575308	0.565792	0.565792	0.556974	0.555762
<i>Nuculana</i> spp.	9.479352	9.518914	9.492364	9.489377	9.495768
<i>S. groenlandicus</i>	0.450951	0.438317	0.435454	0.433683	0.432
<i>Yoldia</i> spp.	7.741715	7.687068	7.633978	7.620898	7.607702
All Taxa	37.14309	36.81878	36.78042	36.72004	36.72434

Table B7: Root mean squared errors of cross-validation comparison of different neighborhood sizes for inverse distance weighting interpolation of abundance.

	10	20	30	40	50
<i>Astarte</i> spp.	0.20076	0.197297	0.194525	0.193801	0.193005
<i>C. ciliatum</i>	0.118508	0.1182	0.118158	0.118092	0.118096
<i>C. crebricostata</i>	0.178445	0.175676	0.175191	0.174917	0.175056
<i>E. tenuis</i>	0.144745	0.142496	0.142143	0.141555	0.141404
<i>L. fluctuosa</i>	0.164014	0.162016	0.161136	0.160368	0.159584
<i>Macoma</i> spp.	0.177266	0.176562	0.176776	0.176684	0.176627
<i>Musculus</i> spp.	0.143827	0.141448	0.141448	0.139244	0.13894
<i>Nuculana</i> spp.	0.209103	0.209976	0.20939	0.209324	0.209465
<i>S. groenlandicus</i>	0.150317	0.146106	0.145151	0.144561	0.144
<i>Yoldia</i> spp.	0.143365	0.142353	0.14137	0.141128	0.140883
All Taxa	0.202231	0.200465	0.200256	0.199928	0.199951

Table B8: Normalized root mean squared errors of cross-validation comparison of different neighborhood sizes for inverse distance weighting interpolation of abundance.

	10	20	30	40	50
<i>Astarte</i> spp.	4.135643	3.99582	3.952543	3.931221	3.913102
<i>C. ciliatum</i>	0.197611	0.198393	0.199003	0.199416	0.199604
<i>C. crebricostata</i>	1.409819	1.387651	1.38495	1.382374	1.382949
<i>E. tenuis</i>	4.860555	4.835613	4.830615	4.817741	4.814614
<i>L. fluctuosa</i>	0.823233	0.815807	0.810672	0.805362	0.801647
<i>Macoma</i> spp.	10.32745	10.21515	10.19067	10.19564	10.17256
<i>Musculus</i> spp.	2.140223	2.106722	2.093356	2.085733	2.082151
<i>Nuculana</i> spp.	5.526878	5.537054	5.538053	5.533416	5.537027
<i>S. groenlandicus</i>	5.443025	5.364335	5.327244	5.303863	5.286878
<i>Yoldia</i> spp.	3.045388	2.991662	2.955523	2.936017	2.929945
All Taxa	18.34854	18.31758	18.28891	18.23963	18.19422

Table B9: Root mean squared errors of cross-validation comparison of different neighborhood sizes for inverse distance weighting interpolation of biomass.

	10	20	30	40	50
<i>Astarte</i> spp.	0.176361	0.170398	0.168552	0.167643	0.16687
<i>C. ciliatum</i>	0.160856	0.161492	0.161989	0.162324	0.162478
<i>C. crebricostata</i>	0.128851	0.126825	0.126578	0.126343	0.126395
<i>E. tenuis</i>	0.141675	0.140948	0.140802	0.140427	0.140336
<i>L. fluctuosa</i>	0.132404	0.131209	0.130383	0.129529	0.128932
<i>Macoma</i> spp.	0.204393	0.202171	0.201686	0.201784	0.201328
<i>Musculus</i> spp.	0.115534	0.113725	0.113004	0.112592	0.112399
<i>Nuculana</i> spp.	0.17667	0.176995	0.177027	0.176879	0.176994
<i>S. groenlandicus</i>	0.157306	0.155032	0.15396	0.153284	0.152793
<i>Yoldia</i> spp.	0.1338	0.13144	0.129852	0.128995	0.128728
All Taxa	0.231985	0.231594	0.231231	0.230608	0.230034

Table B10: Normalized root mean squared errors of cross-validation comparison of different neighborhood sizes for inverse distance weighting interpolation of biomass.

	10	20	30	40	50
<i>Astarte</i> spp.	745.4712	722.7915	714.5806	709.7035	706.307
<i>C. ciliatum</i>	110.0656	110.5008	110.8407	111.0705	111.1755
<i>C. crebricostata</i>	446.9003	434.6509	431.2018	429.3826	428.4615
<i>E. tenuis</i>	2474.21	2466.162	2462.195	2454.771	2452.608
<i>L. fluctuosa</i>	322.108	319.1968	317.2738	315.1086	313.5589
<i>Macoma</i> spp.	5451.449	5384.522	5370.908	5364.969	5347.956
<i>Musculus</i> spp.	1245.61	1226.112	1218.333	1213.896	1211.812
<i>Nuculana</i> spp.	2242.481	2245.677	2244.572	2236.197	2235.773
<i>S. groenlandicus</i>	1950.149	1922.284	1909.263	1901.016	1894.931
<i>Yoldia</i> spp.	2556.478	2510.634	2479.344	2463.131	2457.688
All Taxa	8861.847	8910.511	8880.693	8856.927	8835.425

Table B11: Root mean squared errors of cross-validation comparison of different neighborhood sizes for inverse distance weighting interpolation of calories.

	10	20	30	40	50
<i>Astarte</i> spp.	0.186053	0.180393	0.178343	0.177126	0.176278
<i>C. ciliatum</i>	0.160856	0.161492	0.161989	0.162324	0.162478
<i>C. crebricostata</i>	0.143184	0.139259	0.138154	0.137571	0.137276
<i>E. tenuis</i>	0.14139	0.14093	0.140703	0.140279	0.140155
<i>L. fluctuosa</i>	0.132509	0.131312	0.130521	0.12963	0.128992
<i>Macoma</i> spp.	0.186772	0.18448	0.184013	0.18381	0.183227
<i>Musculus</i> spp.	0.115534	0.113725	0.113004	0.112592	0.112399
<i>Nuculana</i> spp.	0.182884	0.183145	0.183055	0.182372	0.182337
<i>S. groenlandicus</i>	0.157329	0.155081	0.154031	0.153365	0.152874
<i>Yoldia</i> spp.	0.134227	0.13182	0.130177	0.129326	0.12904
All Taxa	0.216883	0.218074	0.217344	0.216762	0.216236

Table B12: Normalized root mean squared errors of cross-validation comparison of different neighborhood sizes for inverse distance weighting interpolation of calories.

APPENDIX C

	<i>Astarte</i> spp.	<i>C. ciliatum</i>	<i>C.</i> <i>crebricostata</i>	<i>E. tenuis</i>	<i>L.</i> <i>fluctuosa</i>	<i>Macoma</i> spp.	<i>Musculus</i> spp.	<i>Nuculana</i> spp.	<i>S.</i> <i>groenlandicus</i>
<i>C. ciliatum</i>	0.998								
<i>C. crebricostata</i>	0.492	0.026*							
<i>E. tenuis</i>	0.303	0.734	0.000*						
<i>L. fluctuosa</i>	1.000	0.981	0.883	0.254					
<i>Macoma</i> spp.	0.001*	0.005*	0.000*	0.588	0.002*				
<i>Musculus</i> spp.	1.000	1.000	0.542	0.956	0.999	0.215			
<i>Nuculana</i> spp.	0.011*	0.053*	0.000*	0.976	0.014*	0.992	0.548		
<i>S. groenlandicus</i>	0.003*	< 0.001*	0.538	< 0.001*	0.058	<0.001*	0.025*	< 0.001*	
<i>Yoldia</i> spp.	0.000*	< 0.001*	< 0.001*	< 0.001*	<0.001*	< 0.001*	< 0.001*	< 0.001*	< 0.001*

Table C1: Results of Tukey's HSD test of gross heats across taxa (p-values). Significant results (p-value < 0.05) are denoted with an asterisk*

Taxon	S (2009)	S (2010)	S (2012)	S (2013)	S (All Years)	K (2009)	K (2010)	K (2013)	K (2013)	K (All Years)
<i>Astarte</i> spp.	0.009	2.620	1.639	1.154	1.821	1.757	8.261	4.532	1.757	8.261
<i>C. ciliatum</i>	n/a	n/a	0.635	0.032	0.831	n/a	n/a	3.571	n/a	n/a
<i>C. crebricostata</i>	0.057	1.867	1.114	0.363	1.638	1.312	7.357	2.305	1.312	7.357
<i>E. tenuis</i>	1.569	0.366	0.551	1.284	0.976	6.251	2.558	3.214	6.251	2.558
<i>L. fluctuosa</i>	0.803	2.227	1.351	0.849	1.317	2.295	8.593	3.681	2.295	8.593
<i>Macoma</i> spp.	2.631	3.509	1.606	2.912	2.505	10.271	20.348	5.871	10.271	20.348
<i>Musculus</i> spp.	n/a	1.727	1.323	0.406	1.638	n/a	4.675	3.517	n/a	4.675
<i>Nuculana</i> spp.	-0.051	0.324	0.503	0.927	0.299	1.638	2.903	2.474	1.638	2.903
<i>S. groenlandicus</i>	n/a	-2.545E- 16	0.896	2.127	4.336	n/a	1.000	2.902	n/a	1.000
<i>Yoldia</i> spp.	3.570	1.233	1.363	3.117	2.561	20.432	4.850	5.154	20.432	4.850

Table C2: Skewness (S) and kurtosis (K) of size frequency-distributions. Taxa with insufficient sample sizes to measure skewness and kurtosis in certain years are denoted by “n/a”

References

- Ambrose, W. G., C. von Quillfeldt, L. M. Clough, P. V. R. Tilney, and T. Tucker. 2005. The sub-ice algal community in the Chukchi Sea: large- and small-scale patterns of abundance based on images from a remotely operated vehicle. *Polar Biology* 28:784–795.
- Arrigo, K. R., and G. L. van Dijken. 2011. Secular trends in Arctic Ocean net primary production. *Journal of Geophysical Research: Oceans* 116:C09011.
- Arrigo, K. R., G. van Dijken, and S. Pabi. 2008. Impact of a shrinking Arctic ice cover on marine primary production. *Geophysical Research Letters* 35:L19603.
- Arrigo, K. R., and D. N. Thomas. 2004. Large scale importance of sea ice biology in the Southern Ocean. *Antarctic Science* 16:471–486.
- Basen, T., D. Martin-Creuzburg, and K.O. Rothhaupt. 2011. Role of essential lipids in determining food quality for the invasive freshwater clam *Corbicula fluminea*. *Journal of the North American Benthological Society* 30:653–664.
- Benedito-Cecilio, E., and M. Morimoto. 2002. Effect of preservatives on caloric density in the muscles of *Hoplias* aff. *malabaricus* (Bloch, 1794) (Osteichthyes, Erythrinidae). *Acta Scientiarum* 24:489–492.
- Beukema, J. J., and R. Dekker. 2005. Decline of recruitment success in cockles and other bivalves in the Wadden Sea: possible role of climate change, predation on postlarvae and fisheries. *Marine Ecology Progress Series* 287:149–167.
- Beukema, J. J., and R. Dekker. 2014. Variability in predator abundance links winter temperatures and bivalve recruitment: correlative evidence from long-term data in a tidal flat. *Marine Ecology Progress Series* 513:1–15.
- Beukema, J. J., R. Dekker, and J. M. Jansen. 2009. Some like it cold: populations of the tellinid bivalve *Macoma balthica* (L.) suffer in various ways from a warming climate. *Marine Ecology Progress Series* 384:135–145.
- Beukema, J. J., R. Dekker, and C. J. M. Philippart. 2010. Long-term variability in bivalve recruitment, mortality, and growth and their contribution to fluctuations in food stocks of shellfish-eating birds. *Marine Ecology Progress Series* 414:117–130.
- Blanchard, A. L., C. L. Parris, A. L. Knowlton, and N. R. Wade. 2013. Benthic ecology of the northeastern Chukchi Sea. Part I. Environmental characteristics and macrofaunal community structure, 2008–2010. *Continental Shelf Research* 67:52–66.
- Bluhm, B. A., and R. Gradinger. 2008. Regional variability in food availability for arctic marine mammals. *Ecological Applications* 18:S77–S96.
- Boetius, A., S. Albrecht, K. Bakker, C. Bienhold, J. Felden, M. Fernández-Méndez, S. Hendricks, C. Katlein, C. Lalande, T. Krumpen, M. Nicolaus, I. Peeken, B. Rabe,

- A. Rogacheva, E. Rybakova, R. Somavilla, and F. Wenzhöfer. 2013. Export of algal biomass from the melting arctic sea ice. *Science* 339:1430–1432.
- Bond, N. A., and J. M. Adams. 2002. Atmospheric forcing of the southeast Bering Sea Shelf during 1995–99 in the context of a 40-year historical record. *Deep Sea Research Part II: Topical Studies in Oceanography* 49:5869–5887.
- Carroll, M. L., and J. Carroll. 2003. The Arctic Seas. Pages 127–156 in K. Black and G. Shimmield, editors. *Biogeochemistry of Marine Systems*. Blackwell Publishing Ltd, Oxford, U.K.
- Clarke, J. T., A. A. Brower, C. L. Christman, and M. C. Ferguson. 2014. Distribution and relative abundance of marine mammals in the northeastern Chukchi and eastern Beaufort Seas, 2013. Annual Report, OCS Study BOEM 2014-018, National Marine Mammal Laboratory, Alaska Fisheries Science Center, NMFS, NOAA, 7600 Sand Point Way NE, F/AKC3, Seattle, WA 98115-6349.
- Clements, J. C., M. Ellsworth-Power, and T. A. Rawlings. 2013. Diet breadth of the northern moonsnail (*Lunatia heros*) on the northwestern Atlantic coast (Naticidae). *American Malacological Bulletin* 31:331–336.
- Clements, J. C., and T. A. Rawlings. 2014. Ontogenetic shifts in the predatory habits of the northern moonsnail (*Lunatia heros*) on the northwestern Atlantic coast. *Journal of Shellfish Research* 33:755–768.
- Cooper, L. W., J. M. Grebmeier, I. L. Larsen, V. G. Egorov, C. Theodorakis, H. P. Kelly, and J. R. Lovvorn. 2002. Seasonal variation in sedimentation of organic materials in the St. Lawrence Island polynya region, Bering Sea. *Marine Ecology Progress Series* 226:13–26.
- Dekker, R., and J. J. Beukema. 2014. Phenology of abundance of bivalve spat and of their epibenthic predators: limited evidence for mismatches after cold winters. *Marine Ecology Progress Series* 513:17–27.
- Dolan, D. M., A. H. El-Shaarawi, and T. B. Reynoldson. 2000. Predicting benthic counts in Lake Huron using spatial statistics and quasi-likelihood. *Environmetrics* 11:287–304.
- Dunton, K. H., J. L. Goodall, S. V. Schonberg, J. M. Grebmeier, and D. R. Maidment. 2005. Multi-decadal synthesis of benthic-pelagic coupling in the western arctic: Role of cross-shelf advective processes. *Deep-Sea Research Part II-Topical Studies in Oceanography* 52:3462–3477.
- Dunton, K. H., J. M. Grebmeier, and J. H. Trefry. 2014. The benthic ecosystem of the northeastern Chukchi Sea: An overview of its unique biogeochemical and biological characteristics. *Deep-Sea Research Part II-Topical Studies in Oceanography* 102:1–8.
- ESRI. 2013a. ArcGIS Help 10.1 - Cross Validation (Geostatistical Analyst).

- ESRI. 2013b. ArcGIS Help 10.1 - Hot Spot Analysis (Getis-Ord Gi*) (Spatial Statistics).
- ESRI. 2013c. ArcGIS Help 10.1 - How Hot Spot Analysis (Getis-Ord Gi*) works.
- Falk-Petersen, S., J. R. Sargent, J. Henderson, E. N. Hegseth, H. Hop, and Y. B. Okolodkov. 1998. Lipids and fatty acids in ice algae and phytoplankton from the marginal ice zone in the Barents Sea. *Polar Biology* 20:41–47.
- Fay, F. H. 1982. Ecology and biology of the Pacific walrus, *Odobenus rosmarus divergens*. *North American Fauna* 74:1–279.
- Fay, F. H., and J. J. Burns. 1988. Maximal feeding depth of walruses. *Arctic* 41:239–240.
- Fay, F. H., B. P. Kelly, P. H. Gehnrich, J. L. Sease, and A. A. Hoover. 1984. Modern populations, migrations, demography, trophics, and historical status of the Pacific walrus. NOAA, U.S. Department of Commerce, Washington D.C., pages 231–376.
- Feder, H., N. Foster, S. Jewett, T. Weingartner, and R. Baxteer. 1994. Mollusks in the northeastern Chukchi Sea. *Arctic* 47:145–163.
- Feder, H. M., S. C. Jewett, and A. L. Blanchard. 2007. Southeastern Chukchi Sea (Alaska) macrobenthos. *Polar Biology* 30:261–275.
- Fox, A. L., E. A. Hughes, R. P. Trocine, J. H. Trefry, S. V. Schonberg, N. D. McTigue, B. K. Lasorsa, B. Konar, and L. W. Cooper. 2014. Mercury in the northeastern Chukchi Sea: Distribution patterns in seawater and sediments and biomagnification in the benthic food web. *Deep Sea Research Part II: Topical Studies in Oceanography* 102:56–67.
- Fujiwara, A., T. Hirawake, K. Suzuki, I. Imai, and S.-I. Saitoh. 2014. Timing of sea ice retreat can alter phytoplankton community structure in the western Arctic Ocean. *Biogeosciences* 11:1705–1716.
- Gerasimova, A. V., and N. V. Maximovich. 2013. Age-size structure of common bivalve mollusc populations in the White Sea: the causes of instability. *Hydrobiologia* 706:119–137.
- Glud, R. N., J. Woelfel, U. Karsten, M. Kühl, and S. Rysgaard. 2009. Benthic microalgal production in the Arctic: applied methods and status of the current database. *Botanica Marina* 52:559–571.
- Grebmeier, J., H. Feder, and C. Mcroy. 1989. Pelagic-benthic coupling on the shelf of the northern Bering and Chukchi Seas 2. Benthic Community Structure. *Marine Ecology Progress Series* 51:253–268.
- Grebmeier, J. M., L. W. Cooper, H. M. Feder, and B. I. Sirenko. 2006a. Ecosystem dynamics of the Pacific-influenced northern Bering and Chukchi Seas in the Amerasian Arctic. *Progress in Oceanography* 71:331–361.

- Grebmeier, J. M., and K. H. Dunton. 2000. Benthic processes in the northern Bering/Chukchi Seas: status and global change. Pages 61–71. US Marine Mammal Commission, Washington, D.C.
- Grebmeier, J. M., J. E. Overland, S. E. Moore, E. V. Farley, E. C. Carmack, L. W. Cooper, K. E. Frey, J. H. Helle, F. A. McLaughlin, and S. L. McNutt. 2006b. A major ecosystem shift in the northern Bering Sea. *Science* 311:1461–1464.
- Grebmeier, J. M., W. O. Smith, and R. J. Conover. 2013. Biological processes on Arctic continental shelves: Ice-ocean-biotic interactions. Pages 231–261 in W. O. S. Jr and J. M. Grebmeier, editors. *Arctic Oceanography: Marginal Ice Zones and Continental Shelves*. American Geophysical Union.
- Gutiérrez, J. L., C. G. Jones, D. L. Strayer, and O. O. Iribarne. 2003. Mollusks as ecosystem engineers: the role of shell production in aquatic habitats. *Oikos* 101:79–90.
- Harding, J. M., S. E. King, E. N. Powell, and R. Mann. 2008. Decadal trends in age structure and recruitment patterns of ocean quahogs *Arctica islandica* from the Mid-Atlantic Bight in relation to water temperature. *Journal of Shellfish Research* 27:667–690.
- Hare, S. R., and N. J. Mantua. 2000. Empirical evidence for North Pacific regime shifts in 1977 and 1989. *Progress in Oceanography* 47:103–145.
- Harsem, Ø., A. Eide, and K. Heen. 2011. Factors influencing future oil and gas prospects in the Arctic. *Energy Policy* 39:8037–8045.
- Hegseth, E. N. 1998. Primary production of the northern Barents Sea. *Polar Research* 17:113–123.
- Himmelman, J., and J. Hamel. 1993. Diet, behavior and reproduction of the whelk *Buccinum undatum* in the northern Gulf of St. Lawrence, eastern Canada. *Marine Biology* 116:423–430.
- Hondolero, D., B. A. Bluhm, and K. Iken. 2012. Caloric content of dominant benthic species from the northern Bering and Chukchi Seas: historical comparisons and the effects of preservation. *Polar Biology* 35:637–644.
- Horner, R., and G. Schrader. 1982. Relative contributions of ice algae, phytoplankton, and benthic microalgae to primary production in nearshore regions of the Beaufort Sea. *Arctic* 35:485–503.
- Hsiao, S. 1992. Dynamics of ice algae and phytoplankton in Frobisher Bay. *Polar Biology* 12:645–651.
- Hunt, G. L., P. Stabeno, G. Walters, E. Sinclair, R. D. Brodeur, J. M. Napp, and N. A. Bond. 2002. Climate change and control of the southeastern Bering Sea pelagic ecosystem. *Deep-Sea Research Part II-Topical Studies in Oceanography* 49:5821–5853.

- Huntington, H. P. 2009. A preliminary assessment of threats to arctic marine mammals and their conservation in the coming decades. *Marine Policy* 33:77–82.
- Jaramillo, J. R., and R. J. Thompson. 2008. The reproductive response of the protobranch bivalve *Yoldia hyperborea* to an intermittent influx of phytodetritus: an experimental approach. *Journal of Experimental Marine Biology and Ecology* 357:57–63.
- Jay, C. V., A. S. Fischbach, and A. A. Kochnev. 2012. Walrus areas of use in the Chukchi Sea during sparse sea ice cover. *Marine Ecology Progress Series* 468:1–13.
- Jay, C. V., J. M. Grebmeier, A. S. Fischbach, T. L. McDonald, L. W. Cooper, and F. Hornsby. 2014. Pacific Walrus (*Odobenus rosmarus divergens*) resource selection in the northern Bering Sea. *PLoS ONE* 9:e93035.
- Konar, B., A. Ravelo, J. Grebmeier, and J. H. Trefry. 2014. Size frequency distributions of key epibenthic organisms in the eastern Chukchi Sea and their correlations with environmental parameters. *Deep Sea Research Part II: Topical Studies in Oceanography* 102:107–118.
- Leu, E., J. E. Søreide, D. O. Hessen, S. Falk-Petersen, and J. Berge. 2011. Consequences of changing sea-ice cover for primary and secondary producers in the European Arctic shelf seas: Timing, quantity, and quality. *Progress in Oceanography* 90:18–32.
- Lewis, D. E., and R. M. Cerrato. 1997. Growth uncoupling and the relationship between shell growth and metabolism in the soft shell clam *Mya arenaria*. *Marine Ecology Progress Series* 158:177–189.
- Lovvorn, J. R., S. E. Richman, J. M. Grebmeier, and L. W. Cooper. 2003. Diet and body condition of spectacled elders wintering in pack ice of the Bering Sea. *Polar Biology* 26:259–267.
- Luchin, V., and G. Panteleev. 2014. Thermal regimes in the Chukchi Sea from 1941 to 2008. *Deep-Sea Research Part II-Topical Studies in Oceanography* 109:14–26.
- Macdonald, R. W., S. M. Solomon, R. E. Cranston, H. E. Welch, M. B. Yunker, and C. Gobeil. 1998. A sediment and organic carbon budget for the Canadian Beaufort shelf. *Marine Geology* 144:255–273.
- Macdonald, T. A., B. J. Burd, V. I. Macdonald, and A. van Roodselaar. 2010. Taxonomic and feeding guild classification for the marine benthic macroinvertebrates of the Strait of Georgia, British Columbia. Page 63. Canadian Technical Report of Fisheries and Aquatic Sciences.
- Macklin, S. A., V. I. Radchenko, S. Saitoh, and P. J. Stabeno. 2002. Variability in the Bering Sea ecosystem. *Progress in Oceanography* 55:1–4.

- Manhas, P., S. Langer, and R. K. Gupta. 2013. Biochemical composition and caloric content of *Paratelphusa masonia* (Henderson), a local freshwater crab, from Jammu waters. *International Journal of Recent Scientific Research* 4:658–661.
- Matheke, G. E. M., and R. Horner. 1974. Primary productivity of the benthic microalgae in the Chukchi Sea near Barrow, Alaska. *Journal of the Fisheries Research Board of Canada* 31:1779–1786.
- McMahon, K. W., W. G. A. Jr, B. J. Johnson, M. Sun, G. R. Lopez, L. M. Clough, and M. L. Carroll. 2006. Benthic community response to ice algae and phytoplankton in Ny Ålesund, Svalbard. *Marine Ecology Progress Series* 310:1–14.
- McTigue, N. D., P. Bucolo, Z. Liu, and K. H. Dunton. 2015. Pelagic-benthic coupling, food webs, and organic matter degradation in the Chukchi Sea: Insights from sedimentary pigments and stable carbon isotopes. *Limnology and Oceanography* 60:429–445.
- McTigue, N. D., and K. H. Dunton. 2014. Trophodynamics and organic matter assimilation pathways in the northeast Chukchi Sea, Alaska. *Deep Sea Research Part II: Topical Studies in Oceanography* 102:84–96.
- Meier, W. N., and J. Stroeve. 2007. Whither Arctic sea ice? A clear signal of decline regionally, seasonally and extending beyond the satellite record. *Annals of Glaciology* 46:428–434.
- Melo, M. T., C. Saturnino, J. N. S. Santos, R. M. Vasconcellos, A. G. Cruz-Filho, and F. G. Araújo. 2010. Correction of the weight and length for juveniles *Atherinella brasiliensis* (Actinopterygii: Atherinopsidae) after fixation in formalin and preservation in ethanol. *Zoologia (Curitiba)* 27:892–896.
- Miller, D. C., R. J. Geider, and H. L. MacIntyre. 1996. Microphytobenthos: The ecological role of the “secret garden” of unvegetated, shallow-water marine habitats. II. Role in sediment stability and shallow-water food webs. *Estuaries* 19:202–212.
- Mills, E., K. Pittman, and B. Munroe. 1982. Effect of preservation on the weight of marine benthic invertebrates. *Canadian Journal of Fisheries and Aquatic Sciences* 39:221–224.
- Mincks, S. L., C. R. Smith, and D. J. DeMaster. 2005. Persistence of labile organic matter and microbial biomass in Antarctic shelf sediments: evidence of a sediment “food bank.” *Marine Ecology Progress Series* 300:3–19.
- Montevecchi, W. A., and J. Piatt. 1984. Composition and energy contents of mature inshore spawning capelin (*Mallotus villosus*): Implications for seabird predators. *Comparative Biochemistry and Physiology Part A: Physiology* 78:15–20.
- National Research Council. 1996. The Bering Sea ecosystem. National Academy Press Washington, DC.

- Neves, R. J., and S. L. Brayton. 1982. Reproductive cycle and associated changes in energy content of body tissues in rainbow trout from the South Fork Holston River, Virginia. Proceedings of the Annual Conference, Southeast Association Fish and Wildlife Agencies 36.
- Overland, J. E., and M. Wang. 2007. Future regional Arctic sea ice declines. Geophysical Research Letters 34:L17705.
- Penney, Z. L., and C. M. Moffitt. 2014. Proximate composition and energy density of stream-maturing adult steelhead during upstream migration, sexual maturity, and kelt emigration. Transactions of the American Fisheries Society 143:399–413.
- Qureshi, N. A., N. U. Saher, R. M. Niazi, and M. A. Gondal. 2008. Effect of different preservatives on the biomass of some selected marine fauna. Pakistan Journal of Zoology 40:249–253.
- Ratkova, T. N., and P. Wassmann. 2005. Sea ice algae in the White and Barents seas: composition and origin. Polar Research 24:95–110.
- Ravelo, A. M., B. Konar, J. H. Trefry, and J. M. Grebmeier. 2014. Epibenthic community variability in the northeastern Chukchi Sea. Deep Sea Research Part II: Topical Studies in Oceanography 102:119–131.
- R Core Team. 2014. R: A language and environment for statistical computing. R Foundation for Statistical Computing, Vienna, Austria. URL <http://www.R-project.org/>.
- Renaud, P. E., A. Riedel, C. Michel, N. Morata, M. Gosselin, T. Juul-Pedersen, and A. Chiuchiolo. 2007. Seasonal variation in benthic community oxygen demand: A response to an ice algal bloom in the Beaufort Sea, Canadian Arctic?. Journal of Marine Systems 67:1–12.
- Richman, S. E., and J. R. Lovvorn. 2003. Effects of clam species dominance on nutrient and energy acquisition by spectacled eiders in the Bering Sea. Marine Ecology Progress Series 261:283–297.
- Rodriguez, C. F., C. Marin-Vindas, F. Chavarria-Solera, R. A. Cruz, and P. Toledo Agtueero. 2011. Seasonal variation in proximate composition of mussels *Tagelus peruvianus* (Bivalvia: Solecurtidae) from the Gulf of Nicoya, Puntarenas, Costa Rica. Revista De Biologia Tropical 59:1517–1523.
- Rysgaard, S., and T. G. Nielsen. 2006. Carbon cycling in a high-arctic marine ecosystem – Young Sound, NE Greenland. Progress in Oceanography 71:426–445.
- Sakshaug, E. 2004. Primary and secondary production in the Arctic Seas. Pages 57–81 in R. Stein and R. W. MacDonald, editors. The Organic Carbon Cycle in the Arctic Ocean. Springer, Berlin.
- Sato, S., T. Chiba, and H. Hasegawa. 2012. Long-term fluctuations in mollusk populations before and after the appearance of the alien predator *Euspira fortunei*

- on the Tona coast, Miyagi Prefecture, northern Japan. *Fisheries Science* 78:589–595.
- Schonberg, S. V., J. T. Clarke, and K. H. Dunton. 2014. Distribution, abundance, biomass and diversity of benthic infauna in the Northeast Chukchi Sea, Alaska: Relation to environmental variables and marine mammals. *Deep Sea Research Part II: Topical Studies in Oceanography* 102:144–163.
- Scolding, J. W. S., C. A. Richardson, and M. J. Luckenbach. 2007. Predation of cockles (*Cerastoderma edule*) by the whelk (*Buccinum undatum*) under laboratory conditions. *Journal of Molluscan Studies* 73:333–337.
- Sheffield, G., F. H. Fay, H. Feder, and B. P. Kelly. 2001. Laboratory digestion of prey and interpretation of walrus stomach contents. *Marine Mammal Science* 17:310–330.
- Sheffield, G., and J. M. Grebmeier. 2009. Pacific walrus (*Odobenus rosmarus divergens*): Differential prey digestion and diet. *Marine Mammal Science* 25:761–777.
- Shields, P. A., and S. R. Carlson. 1996. Effects of formalin and alcohol preservation on lengths and weights of juvenile sockeye salmon. *Alaska Fishery Research Bulletin* 3:81–93.
- Shimek, R. 1984. The diets of Alaskan *Neptunea*. *Veliger* 26:274–281.
- Simpkins, M. A., L. M. Hiruki-Raring, G. Sheffield, J. M. Grebmeier, and J. L. Bengtson. 2003. Habitat selection by ice-associated pinnipeds near St. Lawrence Island, Alaska in March 2001. *Polar Biology* 26:577–586.
- Sirenko, B. I., and V. M. Koltun. 1992. Characteristics of benthic biocenoses of the Chukchi and Bering Seas. Pages 251–258. U.S. Fish and Wildlife Service, Washington, D.C.
- Skazina, M., E. Sofronova, and V. Khaitov. 2013. Paving the way for the new generations: *Astarte borealis* population dynamics in the White Sea. *Hydrobiologia* 706:35–49.
- Smith, L. D., and J. A. Jennings. 2000. Induced defensive responses by the bivalve *Mytilus edulis* to predators with different attack modes. *Marine Biology* 136:461–469.
- Søreide, J. E., E. Leu, J. Berge, M. Graeve, and S. Falk-Petersen. 2010. Timing of blooms, algal food quality and *Calanus glacialis* reproduction and growth in a changing Arctic. *Global Change Biology* 16:3154–3163.
- Stead, R. A., and R. J. Thompson. 2003. The effect of the sinking spring diatom bloom on digestive processes of the cold-water protobranch *Yoldia hyperborea*. *Limnology and Oceanography* 48:157–167.

- Steele, M., W. Ermold, and J. Zhang. 2008. Arctic Ocean surface warming trends over the past 100 years. *Geophysical Research Letters* 35:n/a–n/a.
- Stoker, S. W. 1978. Benthic invertebrate macrofauna of the eastern continental shelf of the Bering and Chukchi Seas. University of Alaska, Fairbanks.
- Strayer, D. L., and H. M. Malcom. 2006. Long-term demography of a zebra mussel (*Dreissena polymorpha*) population. *Freshwater Biology* 51:117–130.
- Stroeve, J. C., M. C. Serreze, M. M. Holland, J. E. Kay, J. Malanik, and A. P. Barrett. 2012. The Arctic's rapidly shrinking sea ice cover: a research synthesis. *Climatic Change* 110:1005–1027.
- Sun, M.-Y., M. L. Carroll, W. G. Ambrose, L. M. Clough, L. Zou, and G. R. Lopez. 2007. Rapid consumption of phytoplankton and ice algae by Arctic soft-sediment benthic communities: Evidence using natural and ¹³C-labeled food materials. *Journal of Marine Research* 65:561–588.
- Sun, M.-Y., L. M. Clough, M. L. Carroll, J. Dai, W. G. Ambrose Jr., and G. R. Lopez. 2009. Different responses of two common Arctic macrobenthic species (*Macoma balthica* and *Monoporeia affinis*) to phytoplankton and ice algae: Will climate change impacts be species specific? *Journal of Experimental Marine Biology and Ecology* 376:110–121.
- Tomczak, M. 1998. Spatial interpolation and its uncertainty using automated anisotropic inverse distance weighting (IDW) - cross-validation/jackknife approach. *Journal of Geographic Information and Decision Analysis* 2:18–30.
- Wacker, A., and E. von Elert. 2004. Food quality controls egg quality of the zebra mussel *Dreissena polymorpha*: The role of fatty acids. *Limnology and Oceanography* 49:1794–1801.
- Walsh, J. J., C. P. McRoy, L. K. Coachman, J. J. Goering, J. J. Nihoul, T. E. Whitledge, T. H. Blackburn, P. L. Parker, C. D. Wirick, P. G. Shuert, J. M. Grebmeier, A. M. Springer, R. D. Tripp, D. A. Hansell, S. Djenidi, E. Deleersnijder, K. Henriksen, B. A. Lund, P. Andersen, F. E. Müller-Karger, and K. Dean. 1989. Carbon and nitrogen cycling within the Bering/Chukchi Seas: Source regions for organic matter effecting AOU demands of the Arctic Ocean. *Progress in Oceanography* 22:277–359.
- Wang, M., and J. E. Overland. 2012. A sea ice free summer Arctic within 30 years: An update from CMIP5 models. *Geophysical Research Letters* 39:L18501.
- Wassmann, P., C. M. Duarte, S. Agustí, and M. K. Sejr. 2011. Footprints of climate change in the Arctic marine ecosystem. *Global Change Biology* 17:1235–1249.
- Wassmann, P., and M. Reigstad. 2011. Future Arctic Ocean seasonal ice zones and implications for pelagic-benthic coupling. *Oceanography* 24:220–231.

- Webster, M. A., I. G. Rigor, S. V. Nghiem, N. T. Kurtz, S. L. Farrell, D. K. Perovich, and M. Sturm. 2014. Interdecadal changes in snow depth on Arctic sea ice. *Journal of Geophysical Research-Oceans* 119:5395–5406.
- Weems, J., K. Iken, R. Gradinger, and M. J. Wooller. 2012. Carbon and nitrogen assimilation in the Bering Sea clams *Nuculana radiata* and *Macoma moesta*. *Journal of Experimental Marine Biology and Ecology* 430–431:32–42.
- Weingartner, T., K. Aagaard, R. Woodgate, S. Danielson, Y. Sasaki, and D. Cavalieri. 2005. Circulation on the north central Chukchi Sea shelf. *Deep Sea Research Part II: Topical Studies in Oceanography* 52:3150–3174.
- Weingartner, T., E. Dobbins, S. Danielson, P. Winsor, R. Potter, and H. Statscewich. 2013. Hydrographic variability over the northeastern Chukchi Sea shelf in summer-fall 2008–2010. *Continental Shelf Research* 67:5–22.
- Wilt, L. M., J. M. Grebmeier, T. J. Miller, and L. W. Cooper. 2013. Caloric content of Chukchi Sea benthic invertebrates: Modeling spatial and environmental variation. *Deep Sea Research Part II: Topical Studies in Oceanography*.
- Woelfel, J., A. Eggert, and U. Karsten. 2014. Marginal impacts of rising temperature on Arctic benthic microalgae production based on in situ measurements and modelled estimates. *Marine Ecology Progress Series* 501:25–40.
- Yunker, M., R. Macdonald, D. Veltkamp, and W. Cretney. 1995. Terrestrial and marine biomarkers in a seasonally ice-covered Arctic estuary - Integration of multivariate and biomarker approaches. *Marine Chemistry* 49:1–50.
- Zettler, M. L. 2002. Ecological and morphological features of the bivalve *Astarte borealis* (Schumacher, 1817) in the Baltic Sea near its geographical range. *Journal of Shellfish Research* 21:33–40.

Vita

Jordann K. Young was born in Austin, Texas. After completing her high school degree in the magnet Science Academy of Lyndon B. Johnson High School in Austin, she attended the University of Texas at Austin, where she earned a Bachelor of Arts degree in Biology, and where she eventually returned to pursue a graduate degree in marine science.

Email address: jkyoung@utexas.edu

This thesis was typed by Jordann K. Young